The Pennsylvania State University

The Graduate School

Department of Chemical Engineering

ENGINEERING THE SOLID-ELECTROLYTE INTERFACE WITH SULFUR-RICH AND CHLROINE-RICH MATERIALS TO PROTECT LITHIUM METAL ANODES FOR LITHIUM-SULFUR BATTERIES

A Dissertation in

Chemical Engineering

by

Michael Regula

Submitted in Partial Fulfillment
of the Requirements
for the Degree of

Doctor of Philosophy

December 2018

The dissertation of Michael Regula was reviewed and approved* by the following:

Michael Janik
Professor of Chemical Engineering
Chair of Committee
Dissertation Co-Adviser

Donghai Wang
Professor of Mechanical Engineering
Dissertation Co-Adviser

Seong Kim
Professor of Chemical Engineering
Professor of Materials Science and Engineering
Head of Chemical Engineering Graduate Program

Sulin Zhang
Professor of Engineering Science and Mechanics and Bioengineering

*Signatures are on file in the Graduate School

ABSTRACT

Humans are becoming increasingly dependent on energy to maintain our quality of life. Our energy generation systems are woefully inefficient, which has significant economic and environmental impacts. More fossil fuels need to be burned to meet energy demand for electricity generation and transportation, while intermittent renewable energy sources, like wind and solar, cannot provide energy in a stable manner. Energy storage devices can stabilize and improve the overall efficiency of electricity generation and transportation. Among energy storage devices, batteries have received the most attention. Specifically, the advent of the lithium-ion battery in 1991 helped spur the portable electronics market and kickstart the production of modern all-electric vehicles. For electric vehicles, though, lithium-ion batteries do not have the energy density nor cost effectiveness to make them pervasive in today's marketplace. A different lithium-based battery chemistry, lithium-sulfur, can meet the energy demands for this application, but many scientific challenges still remain. Sulfur, the high voltage cathode material, is non-conductive and its redox reaction chain with lithium causes rapid drops in battery performance during cycling. Lithium metal, the low voltage anode material, is highly reactive, decomposing electrolyte solvents and lithium-ion conducting salts to form a surface film known as the solid electrolyte interface (SEI). In conventional electrolytes, the SEI composition and morphology is non-uniform across the electrode. Lithium agglomerates during cycling into "dendrite" structures because of non-uniformities in the SEI. Fortunately, the SEI can be engineering with electrolyte additives. In this dissertation, high-sulfur content and high-chlorine content materials are employed as electrolyte additives to protect lithium metal anodes from dendrite formation to enable long-term, stable SEI formation. Well-protected lithium metal anodes directly lead to improvements in lithium-sulfur battery performance. The materials and electrochemical

characterization of these additives should be used to guide future studies in lithium metal anode protection and lithium-sulfur battery development.

TABLE OF CONTENTS

LIST OF FIGURES

ACKNOWLEDGEMENTS

Before getting into the personal acknowledgements, the work in this dissertation was completed using funds from the U.S. Department of Energy and the National Science Foundation. The findings and conclusions do not necessarily reflect the views of either agency.

Now, onto the good stuff.

I saved this section for last and, surprisingly, it has been the most challenging to write. How does one adequately put into words the gratefulness to all the people that made this dissertation possible? Maybe I am just an ungrateful wretch. In any case, here is my best attempt at showing gratitude as I finish my graduate studies and move on to new pursuits.

Dad

I have to start with the man who has been through it all, nearly 27 years and counting. Dad, thank you for your unconditional love. It still blows me away how you were able to support 3 children for nearly 10 years and somehow were able to give each of us your attention 24/7 through that whole time. Five measly years of graduate school is nothing compared to the dedication to raising a family as a single father. Throughout my whole life, you have given me so much support and wisdom that I have relied on to get to this point in my life and career. ("Never buy a new car." You actually did so well, not only have I not bought a new car, I have not bought any cars!) Also, you are the funniest guy I know. Did you ever explore that comedy gig in New Hampshire more? Regardless, thank you for all of the love, guidance, support, and wisdom that you have given me throughout my entire life.

Mom

My father marrying the principal of my elementary school? You mean to tell say that 6th grade me is going to have the ear of the head honcho. I am going to run this school!

That thought lasted a solid 30 seconds. Good times.

Mom, it is that unwavering wisdom to not take advice about running a primary/middle school from a pubescent teen that makes me love you so much. There were quite a few growing pains in the early going, but I am so very thankful you persevered. With Dad, you have helped me to focus my priorities in life, including (but obviously not limited to) remaining faithful to God, recognizing the value of an education, developing fruitful relationships with family and friends, and respecting the Earth on while we live. Thank you for always challenging me to break out of my comfort zone to become a better person.

Sarah

Sarah, thank you for being the best older sister a brother could ask for. I admire how no matter the task in front of you, I always know that you will do your best. "We can win or lose!" That simple phrase famous in our family has had a more profound impact on my life than you will ever know. While I will always have that competitive drive, you have shown me how to be both gracious in victory and defeat, to be able to celebrate the accomplishments of everyone and not just my own. Thank you for being a shining example of how to be a good friend.

Laura

Laura, thank you for being the best younger sister a brother could ask for. Quite simply, your cheerfulness is infectious. In combination with your unparalleled creativity and awareness for the underappreciated in our society, it has and will continue to make you incredible person, both in life and in your career. Also, your ability to be non-judgmental makes it so easy for people to be themselves around you. How many of our conversations have seemingly never-ending fits of laughter? Thank you for your upbeat attitude and for sharing that with the world.

Family, both alive and deceased

I am thankful to be a part of the extensive combined family tree from my parents, having had many great conversations and experiences at family gatherings. I would like to single out a few of them, though, for their impact on my life.

Richard and Marlene Regula

Thank you for being such loving grandparents. You made the nearly 2 hour round trip from Scranton to Mountaintop every day for years when my Dad was a single father to make sure my sisters and I saw family when we arrived home school and during the summers. You continued to show your love after moving to Minnesota by making us feel at home every time we visited. Before by grandmother passed away, she always put her grandchildren before herself. My grandfather carries on her spirit today, showing immense passion for the well-being of his family.

Mary Rudolph

Thank you for being a loving grandparent. Mary, Grammy to us grandchildren, treated us like one of her blood relatives from even before my parents were married. The large family gatherings that would occur at her home further illustrated her welcoming nature. Even has dementia began to wear on her at the end of her life, this quality never wavered. Thank you, Grammy, setting the example of how to be welcoming to others.

Mary and Will Stockdell

Thank you for being a loving aunt and uncle. Aunt Mary needed a double lung transplant in the mid-2000s, a crazy turn of events given her excellent physical health before the transplant, demonstrated by being expert baton twirler. Despite frequent visits to the Mayo Clinic after the surgery, she made remarkable efforts to make her nieces and me feel at home on visits to Minnesota. Her perseverance through all of the seemingly random turmoil in her life is something I continue to truly admire. I also thank my Uncle Will for being dedicated to her to the end.

Dr. Donghai Wang

Thank you, Dr. Wang, for inviting me to join your lab. As your first chemical engineering student at Penn State, there were some unique obstacles to overcome to make this partnership successful. Your combination of creative research directions and entrepreneurial spirit have guided the work in this dissertation and my outlook on the field of energy storage. The College of Engineering's Diefenderfer Fellowship that I was awarded in 2016 highlight not only my technical research abilities, but also your talents as a research advisor. Additionally, you gave me the opportunity to develop me leadership abilities as the laboratory safety manager, giving me to freedom to develop and implement policies to maintain a culture based on safety. Thank you for pushing me to be the best researcher and leader I can be.

Dr. Michael Janik

Thank you, Dr. Janik, for more being a course of academic guidance and support for the last 7 years. As my undergraduate thesis advisor, you helped cultivate my interests in energy research. Your invitation to spend the summer in the REU program in 2012 turned into one of the best experiences of my life. When I told you about my desire to pursue more experimental work in graduate school, you helped me contact Dr. Wang and help us through the logistics of getting my PhD in chemical engineering. You have always been someone I have felt comfortable talking to not only about research, but also about my interests beyond the lab. Thank you for all the doors that you have opened for me during my time at Penn State.

Dr. Seong Kim and Dr. Sulin Zhang

Thank you for serving on my dissertation committee. The feedback I received from both of you after my comprehensive exam helped to guide my next three years of research. I hope that you continue to be an integral part of my career beyond graduate school.

Friends

This section could be as long as all my dissertation chapters combined. From high school through my whole time at Penn State, I have had the opportunity to get to know so many great people. In graduate school alone, I have met so many people through the ChE GSA, through Philanthropic Fantasy Sports, through multiple volleyball leagues, through friends of friends, and so on. For fear of forgetting any single person at this time, expect me to contact each one of you individually to express my gratitude for your friendship.

Chapter 1

Introduction

The U.S. Energy Administration projects a 28% increase in world energy consumption between 2015 and 2040, sparked by economic growth in previously slow developing regions.[1] Both public and private enterprises worldwide are tasked with meeting this energy demand to sustain the vast technological developments since the Industrial Revolution. An additional challenge to meeting this increasing energy demand is doing so in an environmentally-sustainable manner, since our current energy consumption habits are the driving factor of climate change.[2]

Electricity generation and transportation make up approximately 67% of the energy consumption in the United States as of 2017 (65.3 quads). Of that amount, a staggering 71.8% of it gets lost as waste (46.9 quads).[3] It should come as no surprise, then, that both electricity generation and transportation are the two biggest sources of energy inefficiency. For conventional power plants and vehicles, this inefficiency comes from the devices used to power them, namely the steam turbine and the internal combustion engine. These technologies have an efficiency of around 20%-40%, disappointing given that these technologies are primarily powered by fossil fuels.[4]-[5] For renewable energy technologies, like wind and solar, inefficiency comes partially due their dependent devices, but also the intermittency of the power source itself.[6][7] This instability is a major issue for power plants since humans use more energy at certain times in the day. If the sun is not shinning or the wind is not blowing during these peaks hours, operators need to revert back to fossil fuel sources to meet demand. Conversely, if the sun is shining or the wind is blowing during at non-peak hours, the energy generated unused. Any technological developments to recover lost energy would be a boon to the quality-of-life around the world.

Batteries are one important energy storage technology that has received significant attention to help improve the efficiency of our energy systems; for example a battery could store any overages produced during non-peak electricity use for peak hours.[8] Converting chemical energy into electrical energy, batteries take advantage of differences in the electrochemical potentials inherent to every material to drive an electric current to power devices. A high voltage electrochemical reaction occurs at the "cathode", while a low voltage electrochemical reaction occurs at the "anode". This voltage difference is one of two factors that determines a battery's energy.[9]

The second factor is "capacity", the amount of charge stored in the battery. Capacity not only depends on the electrochemical reactions at the anode and cathode, but also on other battery components, such as the separator, current collector, and electrolyte.[10]-[11] The separator provides a barrier between the cathode and the anode materials while the current collector enables the flow of electrons from the cathode/anode to devices. The electrolyte enables the electrochemical reactions at the cathode and anode by providing a medium for the flow of ions that balances the charge of the flow of electrons.[11] Battery researchers, therefore, need to identify not only materials with high and low voltages, but also compatible materials to achieve a high capacity, and, in turn, a high energy density (Figure 1-1).

Battery design does not stop there, however. The next consideration is "cyclability", the number of times the battery can be charged and discharged while maintaining a stable energy density. Consider two examples of batteries that are used extensively today: the alkaline battery and the lead-acid battery. Traditional alkaline batteries do not have any cyclability; referred to as "primary batteries", they are discharged once and discarded.[12] On the other hand, lead-acid batteries, used extensively to power automobiles since the Model T, are powered by electrochemical reactions that are reversible. Because the reactions are reversible, lead-acid batteries are referred to as "secondary batteries."[13]-[14] With sustainability becoming more and

Figure 1-1. A diagram of a lithium-based battery. Many different materials have been proposed for the anode, cathode, and electrolyte for next generation batteries.

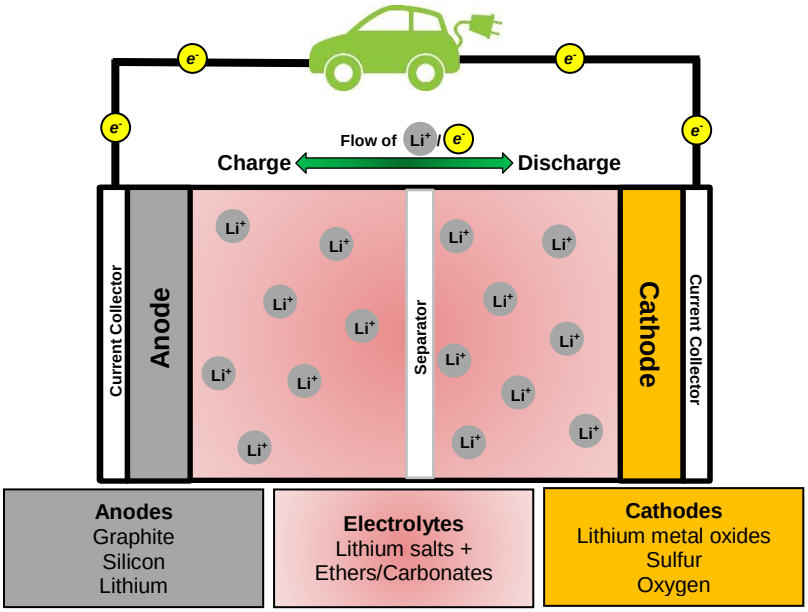

more of a major design goal in the 21st century, the vast majority of research efforts have focused on secondary batteries, attempting to increase their energy density while cycling them thousands of times.

Lithium-ion batteries

Incorporating lithium into batteries had long been a goal of battery researchers. Lithium exhibits both the lowest density and electrochemical potential of any metal that researchers have studied to date. Additionally, the lithium-ion is the smallest of the monovalent ions, a key attribute that has impacted the design of cathodes, anode, and electrolytes.[15]

In the 1980s, multiple breakthroughs enabled lithium to be viably incorporated into batteries for the first time. John Goodenough and Ned Godshall demonstrated a secondary lithium-ion battery dependent on "intercalation" chemistry with lithium cobalt oxide ($LiCoO_2$), a cathode material.[16]-[17] Intercalation refers to process by which a material reversibly inserts

Figure 1-2. The percentage of sales for rechargeable batteries worldwide from 1991 to 2007. (U.S. Geological Survey Circular)

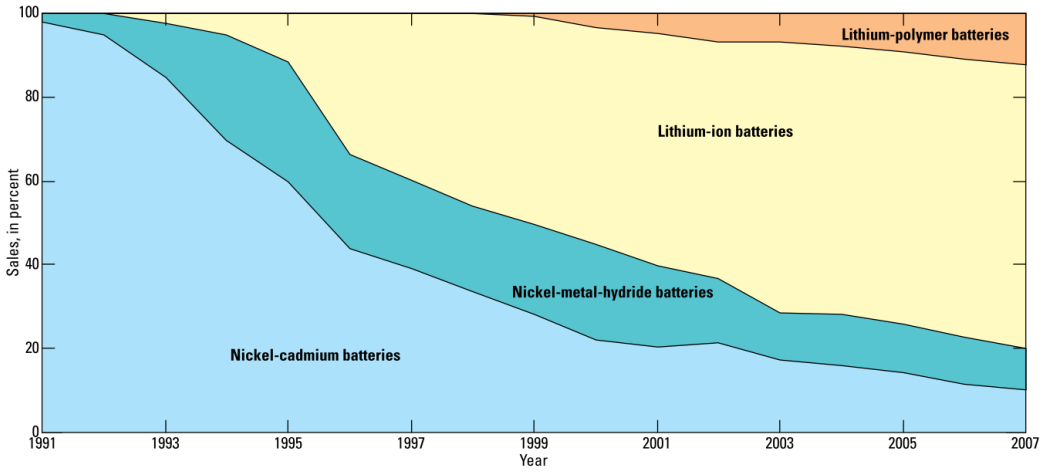

into a layered structure. In the case of $LiCoO_2$, the Li^+ ion is reversibly inserted and removed from the crystal layers of $LiCoO_2$ during cycling. Goodenough and Godshall's work would grow to include numerous transition metal oxides ($LiMn_2O_4$, Li_2MnO_3, $LiFeO_2$, and others), each demonstrating the same highly-reversible intercalation chemistry.[18]-[21] Then, graphite, a low voltage material, was shown to accommodate Li^+ through the same intercalation mechanism. Lithium transition metal oxides and graphite were used in the first commercialized lithium-ion battery (LIB) in 1991.[22] This configuration is widely used in portable electronics today.

By 2007, lithium-based batteries made up 80% of the market for rechargeable batteries (Figure 1-2).[1] By 2002, more than 90% of laptops contained LIBs. Cell phones and hybrid electric vehicles shortly thereafter adopted LIBs or their relative, lithium-polymer batteries, a configuration with a solid-state electrolyte that improves safety. Today and in the future, lithium-based batteries will continue to permeate into new markets.

Lithium-sulfur batteries

These new markets include all-electric vehicles. The primary issue with LIBs based on intercalation chemistry is that they do not have the energy density for electric vehicles to match

the driving range of vehicles with internal combustion engines.[23] To tackle this problem, another lithium-based battery has been extensively investigated: lithium-sulfur (Li-S). Discovered even before the concept of LIBs, Li-S batteries depend on conversion reactions instead of intercalation, reducing sulfur to lithium sulfide.[23]-[24] The overall electrochemical discharge reaction is as follows:

$$S_8 + 16\ Li^+ + 16\ e^- \rightarrow 8\ Li_2S \quad \text{(Eq. 1)}$$

Sulfur occurs naturally as a cyclic octatomic molecule, hence "S_8" as the reactant. In addition to readily reacting with lithium, sulfur is both naturally abundant and an underutilized waste product of many industrial applications.

As a cathode material, sulfur has a theoretical capacity that is more than 10 times higher than lithium metal oxides. When paired with a lithium metal anode, the theoretical gravimetric energy density of lithium-sulfur batteries is 6 times higher than their counterparts. Obtaining performance near those theoretical values, though, has been an issue for researchers for over 50 years.[23]

Challenges for lithium-based batteries

Two major changes to current LIBs would revolutionize the industry: replacing both graphite with lithium metal in the anode and lithium metal oxides with sulfur in the cathode. In order to accomplish that, though, some fundamental scientific obstacles need to be overcome.

Anodes - Graphite to lithium metal

Graphite's intercalation capabilities have carried LIBs into the 21st century. The key drawback, though, is that it has a limited capacity, 372 mAh/g. Compare that to its potential

replacement, lithium metal, which has a capacity of 3860 mAh/g. As mentioned previously, lithium metal is also an attractive anode material because of its low electrochemical potential, weight, and density.[15], [25]

Many electrolyte materials have been studied for lithium metal anodes, but none have obtained commercial success. Common liquid electrolyte solvents, commonly carbonate or ether-based, readily decompose both upon contact with lithium and during cycling. The decomposition of the electrolyte forms a solid-electrolyte interface (SEI) on the lithium metal surface.[26]-[28] While not inherently detrimental to performance, continuous, uncontrolled build-up of this interface leads to an increase in resistance and rapid capacity fading. Moreover, during cycling, lithium particles tend to agglomerate into structures known as "dendrites", which have a thin, branched morphology that, over time, can readily puncture the separator and short-circuit the battery.[28]

Cathodes - Lithium metal oxides to sulfur

Like graphite, the intercalation chemistry for hosting lithium in lithium metal oxides limits their theoretical specific capacity. Transition metals, and thus lithium metal oxides, are also more expensive than many other potential cathode materials, like sulfur.

While OXIS Energy commercialized a Li-S battery in 2015, wide-spread adoption is not imminent given the litany of problems with using the technology. For one, sulfur has an electronic conductivity of 1×10^{-15} S/m (nearly eight orders of magnitude lower than the most insulating semiconductor); therefore, in order to use it as a rechargeable battery material, a conductive material (carbon or a metal) must be added to sulfur.[29]-[31] By adding a non-electrochemically active component, concessions are made that limits the maximum achievable energy density. Even with conductive materials, sulfur's insulating behavior makes it difficult to

fully reverse the electrochemical reaction shown in Eq. 1. Any material lost results in capacity fading in subsequent cycles.

Secondly, sulfur undergoes an approximately 80% volume expansion upon lithiation. Upon expansion, conductive networks lose their structural integrity if sulfur is too tightly packed in the cathode structure. Void space can be engineered into the sulfur-containing structure, but such a concession results in yet another loss in potential energy density.[32]-[34]

Finally, the reaction of sulfur with lithium is not as trivial as the overall electrochemical reaction shown in Eq. 1, with complications arising from reaction intermediates (Figure 1-3).[35] The reduction reaction of sulfur with lithium is typically illustrated via a two-step mechanism, reflected in the charge-discharge profile by two plateaus. Upon discharge, S_8 reduces to long-chain polysulfides (Li_2S_x, $x \geq 3$); then the polysulfides further reduce to short-chain sulfides (Li_2S and Li_2S_2). This reaction mechanism poses a number of engineering challenges. For one, long-chain polysulfides are soluble in Li-S compatible electrolytes, typically ether-based. Polysulfide dissolution causes a phenomenon known as the "shuttle effect", whereby these species react continuously with both the cathode and the anode. This occurs because polysulfides have the ability to disproportionate with one another, reacting and dissociating with themselves. The prevalence of this phenomenon means that Li-S cannot successfully recharge without significant electrode and electrolyte engineering. For another, the short-chain sulfide end products of the reaction mechanism are both insoluble in ether electrolytes and nonconductive. Rather than recharging to form lithium, these species

Figure 1-3. A representative charge-discharge profile for a Li-S battery. The electrochemical reaction of lithium and sulfur proceeds through a series of intermediates. The reaction rate decreases as the order fo the sulfides decreases. Sulfide species also have ability to disproportionate, a property that causes the "polysulfide shuttle effect." (Lu *et al.*)

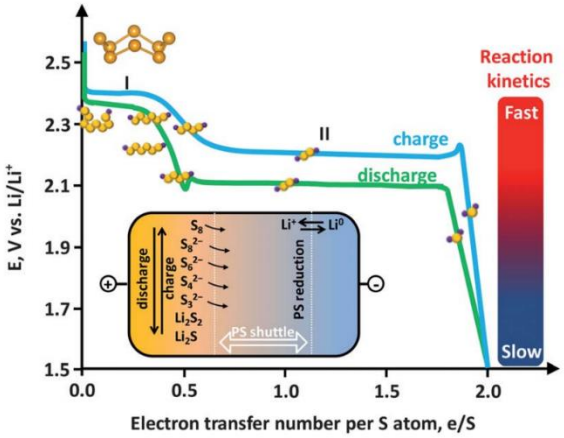

deposit on the electrodes, decreasing their conductivity and increasing the polarization of the cell. Lastly, sulfur species typically corrode lithium metal anodes, inhibiting stable cycling.[36]-[38]

Proposed solutions

A high-level challenge for Li-S batteries is finding electrolyte materials that are compatible with both sulfur species and lithium metal. The goal is to build a uniform, ionically conductive SEI on lithium's highly reactive surface while also mitigating the detrimental effects of polysulfide shuttling.

My work attempts to better understand the fundamentals of SEI formation on lithium metal surfaces in sulfur-containing environments. With that understanding, novel electrolyte materials and compositions were proposed to demonstrate how the SEI could be manipulated to protect lithium metal with the goal of improving Li-S battery performance. Through extensive characterization, high-sulfur and high-chlorine content materials were shown to produce stable SEI layers that were mechanically robust and ionically conductive. The studies that follow demonstrate exciting new research pathways to bring us another step closer to making Li-S batteries the standard in the industry and meeting our ever increasing energy needs.

References

[1] EIA, *U.S. Energy Inf. Adm.* **2017**, *IEO2017*, 143.

[2] P. Poizot, F. Dolhem, *Energy Environ. Sci.* **2011**, *4*, 2003.

[3] U.S. Energy Information Administration, *Monthly Energy Review – April 2018*, **2018**.

[4] E. H. J. N.P. Padture, M. Gell, *Mater. Sci.* **2002**, *296*, 280.

[5] A. K. Agarwal, *Prog. Energy Combust. Sci.* **2007**, *33*, 233.

[6] P. J. Hall, E. J. Bain, *Energy Policy* **2008**, *36*, 4352.

[7] N. S. Lewis, D. G. Nocera, *Proc. Natl. Acad. Sci. U. S. A.* **2006**, *103*, 15729.

[8] M. Armand, J.M. Tarascon, *Nature* **2008**, *451*, 2.

[9] B. Dunn, H. Kamath, J. Tarascon, B. Dunn, H. Kamath, **2011**, *334*, 928.

[10] M. Winter, R. J. Brodd, *Chem. Rev.* **2004**, *104*, 4245.

[11] K. Xu, *Chem. Rev*. **2004**, *104*, 4303.

[12] E. Peled, *J. Electrochem. Soc.* **1979**, *126*, 2047.

[13] R. M. Dell, *Solid State Ionics* **2000**, *134*, 139.

[14] F. Cheng, J. Liang, Z. Tao, J. Chen, *Adv. Mater.* **2011**, *23*, 1695.

[15] D. Lin, Y. Liu, Y. Cui, *Nat. Nanotechnol.* **2017**, *12*, 194.

[16] K. Mizushima, P. C. Jones, P. J. Wiseman, J. B. Goodenough, *Solid State Ionics* **1981**, *3-4*, 171.

[17] N. A. Godshall, *Solid State Ionics* **1986**, *18-19*, 788.

[18] M. M. Thackeray, W. I. F. David, P. G. Bruce, J. B. Goodenough, *Mater. Res. Bull.* **1983**, *18*, 461.

[19] M. M. Thackeray, P. J. Johnson, L. A. de Picciotto, P. G. Bruce, J. B. Goodenough, *Mater. Res. Bull.* **1984**, *19*, 179.

[20] D. Rong, Y. Il Kim, T. E. Mallouk, *Inorg. Chem.* **1990**, *29*, 1531.

[21] M. M. Thackeray, W. I. F. David, J. B. Goodenough, *Mater. Res. Bull.* **1982**, *17*, 785.

[22] Y. Nishi, *J. Power Sources* **2001**, *100*, 101.

[23] P. Bruce, S. Freunberger, *Nat. Mater.* **2012**, *11*, 19.

[24] Y.-X. Yin, S. Xin, Y.-G. Guo, L.-J. Wan, *Angew. Chem. Int. Ed. Engl.* **2013**, *52*, 13186.

[25] Y. Guo, H. Li, T. Zhai, *Adv. Mater.* **2017**, *29*, 1.

[26] L. J. Fu, H. Liu, C. Li, Y. P. Wu, E. Rahm, R. Holze, H. Q. Wu, *Solid State Sci.* **2006**, *8*, 113.

[27] Y. Lu, Z. Tu, L. A. Archer, *Nat. Mater.* **2014**, *13*, 961.

[28] F. Wu, J. Qian, R. Chen, J. Lu, L. Li, H. Wu, J. Chen, T. Zhao, Y. Ye, K. Amine, *ACS Appl. Mater. Interfaces* **2014**, *6*, 15542.

[29] X. Ji, K. T. Lee, L. F. Nazar, *Nat. Mater.* **2009**, *8*, 500.

[30] J. Song, Z. Yu, T. Xu, S. Chen, H. Sohn, M. Regula, D. Wang, *J. Mater. Chem. A* **2014**, *2*, 8623.

[31] J. Song, T. Xu, M. L. Gordin, P. Zhu, D. Lv, Y.-B. Jiang, Y. Chen, Y. Duan, D. Wang, *Adv. Funct. Mater.* **2014**, *24*, 1243.

[32] D. Li, F. Han, S. Wang, F. Cheng, Q. Sun, W.-C. Li, *ACS Appl. Mater. Interfaces* **2013**, *5*, 2208.

[33] G. Zheng, Y. Yang, J. J. Cha, S. S. Hong, Y. Cui, *Nano Lett.* **2011**, *11*, 4462.

[34] H. Yamin, A. Gorenshtein, J. Penciner, Y. Sternberg, E. Peled, *J. Electrochem. Soc.* **1988**, *135*, 1045.

[35] J. Akridge, *Solid State Ionics* **2004**, *175*, 243.

[36] Y. V Mikhaylik, J. R. Akridge, *J. Electrochem. Soc.* **2004**, *151*, A1969.

[37] Y. Diao, K. Xie, S. Xiong, X. Hong, *J. Electrochem. Soc.* **2012**, *159*, A421.

[38] T. A. Pascal, K. H. Wujcik, D. R. Wang, N. P. Balsara, D. Prendergast, *Phys Chem Chem Phys* **2017**, *19*, 1441.

Chapter 2

Trichloropropane-based sulfur polymer interlayer improves the columbic efficiency of lithium metal anodes

Abstract

Lithium metal anodes offer improved gravimetric and volumetric energy density that would revolutionize the battery industry. The practical application of Li metal, however, is hindered by the dendrite growth and low Li deposition/stripping Coulombic efficiency (CE). Here, we used sulfur-rich polymer as an electrolyte additive to suppress the dendrite growth and improve the CE of lithium metal. The sulfur-rich polymers were synthesized *via* a facile emulsion-catalyzed reaction between 1,2,3-trichloropropane and lithium polysulfides. The highest sulfur content polymer (83.7 wt%) produced a uniform solid electrolyte interphase consisting of both organic and inorganic sulfides. This fortified SEI enabled a >97% lithium deposition/stripping efficiency over 300 cycles in Li/stainless steel coin cells. Additionally, a low, stable voltage hysteresis (~ 50 mV) illustrated lower resistance through the enhanced interface.

Introduction

Lithium-ion batteries (LIBs) have been the standard for energy storage for nearly 25 years, catalyzing the portable electronics market.[1] State-of-the-art LIBs depend on intercalation chemistry, in which the Li^+ ion inserts between the layers of metal oxides (cathode) and graphite (anode) during cycling. This process is highly reversible, allowing for reliable long-term cycling. The main issue, though, is that batteries made with these intercalation electrode materials do not

have the energy density necessary to be widely adopted for electric vehicles and grid-level energy storage systems, the next major frontier in battery technologies.[2]-[3]

Focusing specifically on the anode, graphite has a specific capacity of around 370 mAh g^{-1}. Comparatively, lithium metal exhibits a specific capacity of 3860 mAh g^{-1}.[4] Because lithium metal has both a low mass (6.94 g mol^{-1} molecular weight) and density (0.53 g cm^{-1}), this 10-fold increase in specific capacity could translate into a similar-fold increase in energy density.[5]-[6] Using lithium metal as an anode, though, still requires significant engineering of the solid electrolyte interphase (SEI), the surface film that spontaneously forms on the electrode surface through active material and electrolyte decomposition and then changes during battery cycling.[4]-[7] For most batteries, the electrolyte primarily consists of a carbonate [8]-[16] or ether [17]-[35] solvent and a lithium salt. These components all decompose to form a complex passivating film on lithium metal.[17] Only employing the solvent and supporting salt, this passivating film unsustainably builds up on the lithium metal surface after each deposition/stripping cycle.[18]-[19] The telltale sign of unsustainable SEI growth is the formation of lithium metal "dendrites", which are protruding, branched agglomerations of inactive lithium that grow to puncture the separator, causing short circuits and making the battery hazardous.

Dendrite formation can be suppressed by employing electrolyte additives. Mikhaylik first showed in 2008 that adding lithium nitrate ($LiNO_3$) to the electrolyte reduced the rate of self-discharge in Li-S batteries.[20] Aurbach et al. then proceeded to characterize the decomposition products of $LiNO_3$ in a polysulfide environment, specifically showing how $LiNO_3$ reduces to Li_xNO_y while also oxidizing polysulfides to Li_xSO_y.[21] More recent work from the Cui group demonstrated how $LiNO_3$ and long-chain lithium polysulfides work together to limit the decomposition of LiTSFI, evidenced by a significant decrease in the $–CF_3$ peak in both the C 1s and F 1s XPS spectra. This effect produced a flat SEI morphology with significantly fewer nucleation sites compared to only using $LiNO_3$ for surface protection.[22] The Zhang group

demonstrated the need to properly tune the polysulfide concentration to slow the consumption of the organic electrolytes in conjunction with $LiNO_3$.[23]

Relying heavily on polysulfides for lithium metal protection, however, does not address some of the fundamental issues of using polysulfides in the first place, one of which is that polysulfides corrode lithium metal over time. Our group explored how organosulfide materials behave as a polysulfide carriers that forms a SEI layer with both organic and inorganic components. This hybrid SEI has the elasticity to constrain dendrite formation.[24]-[26] Many sulfur-rich polymers have been proposed as cathode materials, synthesized via facile methods such as "inverse vulcanization" [27]-[28] and emulsion polymerization [29], but only our group has investigated their effectiveness for stable SEI formation.

We further investigate these sulfur-rich polymers in this study. Polymers based on 1,2,3-trichloropropane (TCP) were synthesized using a facile emulsion-based synthesis technique. The length of the sulfur chains in the polymer can be well-controlled using this technique, allowing for a systematic study of the impacts of the organic and inorganic decomposition products from the polymer. The highest sulfur-content polymer (83.7 wt%), TCP-S_8, demonstrated the best ability to suppress Li dendrite formation, creating a uniform and unbroken SEI. Stable lithium deposition/stripping, studied with efficiency and voltage hysteresis measurements in Li|stainless steel cells, occurs for approximately 400 cycles using TCP-S_8 with an improved average Coulombic efficiency (CE) of 97.3%. The exceptional SEI stability coupled with the facile synthesis technique of the TCP-based polymers offers unique insights to move closer to commercializing lithium metal-based batteries.

Experimental Methods

Preparation of polymers

An emulsion-based procedure similar to the one employed by Lim et al. was used to synthesize the TCP-S_x polymers.[36] A lithium polysulfide solution was first prepared by adding lithium sulfide (Li_2S, 99.9%, Alfa Aesar) and sulfur (99.5%, Alfa Aesar) to N,N-dimethylformamide (DMF, 99.8%, Sigma-Aldrich) in an argon-filled glove box. The amount of sulfur was varied to produce lithium polysulfides of order between 2 and 8, which would then produce a polymer with the respective chain length order (though the chain length could vary from chain to chain due to polysulfide disproportionation).[37] The polysulfide solution was stirred at room temperature until the lithium polysulfides were fully dissolved in DMF. Hexadecyltrimethylammonium bromide (CTAB, $\geq$ 98%, Sigma-Aldrich) was then added as a phase transfer catalyst and stirred until it, too, dissolved in DMF. 1,2,3-trichloropropane (TCP, 99%, Sigma-Aldrich) was then added to the solution and stirred for 8 hours. The amount of TCP added was governed by the stoichiometry of the conversion reaction between the lithium polysulfides and TCP. During the course of the reaction with TCP, the solution turned from a deep red to light red. The solution was then decanted and then centrifuged three times in distilled water to remove the unreacted species. The solid products were then dried in a convection oven at 70^{o}C overnight.

Characterization

The raw TCP-S_x polymers and the SEI layer containing these polymers were characterized using X-ray diffraction (XRD), Fourier-transform infrared spectroscopy (FTIR), X-ray photoemission spectroscopy (XPS), scanning electron microscopy (SEM), and energy-dispersive X-ray spectroscopy (EDS). The XRD pattern was obtained with Cu-K_α radiation on a Rigaku

Miniflex II. The diffraction pattern was determined between 10-80^{o} 2Θ at a scan rate speed of 0.1^{o} per minute. FTIR spectra were conducted using a Bruker VERTEX 70v using the diamond attenuated total reflectance (ATR) accessory. XPS spectra were collected on a PHI *VersaProbe* II Scanning XPS Microprobe. SEM/EDS was run on a FEI Quanta 200 to determine the morphology of the SEI formed on stainless steel and lithium metal from lithium deposition/ stripping. Air-sensitive containers were used to transfer samples from cycled cells to and from each piece of characterization equipment when appropriate.

Electrochemical measurement

Lithium deposition tests and cyclic voltammetry were run on Neware battery testers and CH Instruments, respectively, using 2016 coin cells at room temperature. For the deposition tests, lithium metal was deposited on stainless steel at a constant current rate. Lithium was then stripped from the stainless steel, also at a constant current rate, until the voltage reached 0.5 V vs. Li/Li^{+} (all voltages referenced to Li/Li^{+} unless otherwise noted). Time governed the capacity of lithium deposited and stripped. For cyclic voltammetry tests, the potential window was between -0.5 V and 5 V, swept at a 1 mV sec^{-1} rate. The synthesized TCP-S_x powder was added between the Celegard separator and lithium metal. The electrolyte used was 1M lithium bis(trifluoromethanesulfonyl)imide (LiTFSI, BASF) in 1:1v 1,3-dioxolane (DOL, BASF) and 1,2-dimethoxyethane (DME, BASF) with 4 wt% lithium nitrate ($LiNO_3$, 99.99% trace metals basis, Sigma-Aldrich) and 2.5 wt% of the TCP-S_x polymer . Cells and electrolyte were prepared in an MBraun argon-filled glove box with H_2O and O_2 less than 1 ppm.

Results and Discussion

Polymer synthesis

We successfully synthesized TCP-S_x polymers with $2 \leq x \leq 8$ through an emulsion-catalyzed reaction described in Figure 2-1a. We focused on studying the polymers that have sulfur chain lengths primarily of x = 2, 5, and 8 to determine the effects of sulfur content on the stability of the SEI. The emulsion synthesis method produces nano-sized, nearly spherical polymer particles (Supplementary Figure A-1). The x-ray diffraction (XRD) pattern (Supplementary Figure A-2) for the TCP-S_x polymers illustrated an amorphous particle structure. The broad peak in the polymer samples between 20° and 25° represents the successful synthesis of carbon-based nanoparticles.[38] There were no peaks representative of elemental sulfur, suggesting all of the sulfur reacted with TCP. Elemental analysis determined that TCP-S_2, TCP-S_5, and TCP-S_8 had a sulfur content of 61.92 wt%, 79.70 wt%, and 83.70 wt%, respectively (Supplementary Figure A-3). Fourier transform infrared spectroscopy (FT-IR) demonstrated that pure TCP exhibits strong peaks in between both 600 – 800 cm^{-1}, which can be attributed to C-Cl stretching.[38] These peaks disappear after reacting with lithium polysulfide, indicating the removal of the chlorine atoms from TCP (Supplementary Figure A-4). Elemental sulfur was used to reference the S-S bond peak at around 490 cm^{-1}. The strength of this S-S peak increases as the sulfur chain length in the polymer increases.[39] When the sulfur-rich polymers are added into the electrolyte and cycled, the S-S bonds react electrochemically with lithium. This reaction produces two types of sulfides: inorganic ($Li_2S/Li_2S_2/Li_2S_x$) and organic (RS_xLi_3) (Figure 2-1b). SEIs with inorganic sulfides have previously been shown to limit the decomposition of LiTFSI, while SEIs with organic sulfides demonstrate

Figure 2-1. a) The emulsion-catalyzed substitution reaction of 1,2,3-trichloropropane (TCP) and lithium polysulfides to form a sulfur-rich polymer. b) The reaction of the TCP-S_x polymer with lithium metal to form organic polysulides, inorganic polysulfides, and inorganic sulfides. c) Illustration of the SEI morphology on lithium metal with organic and inorganic components.

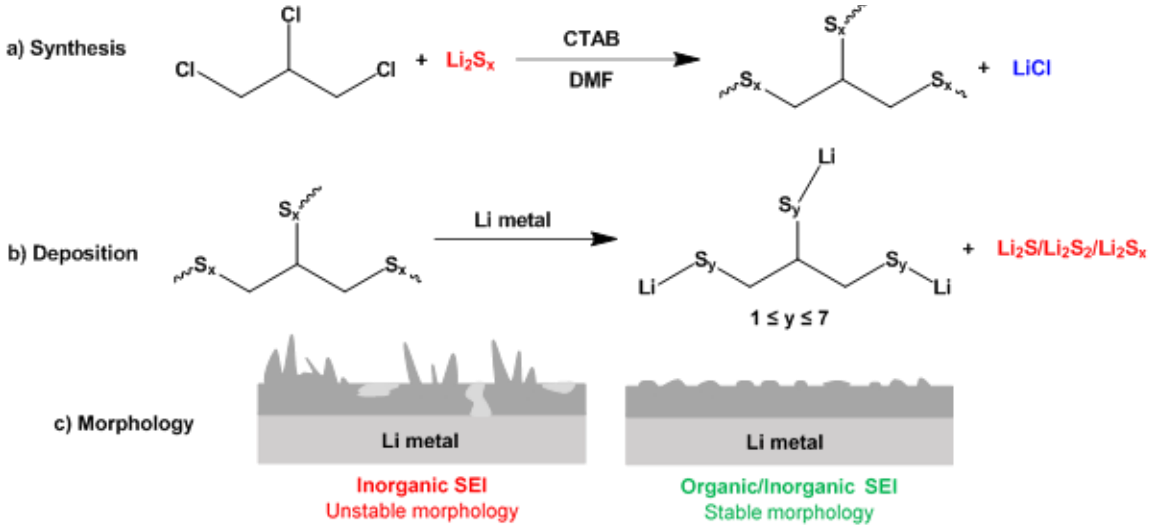

improves flexibility and stability.[22][26] These components work together in a hybrid SEI layer to suppress lithium dendrite formation (Figure 2-1c).[26]

Characterization of the SEI

Stable SEI layers are critical for the suppression of Li dendrites and enhancement of Li deposition/stripping CE. The stability of the hybrid SEI and dendrite-free lithium metal after 50 cycles (where stainless steel was used as the working electrode for Li deposition/stripping) was illustrated using SEM and EDS (Figure 2-2). Large cracks are observed in the SEI on the stainless steel electrode using just $LiNO_3$ as an additive (Figure 2-2a), indicating the breaking of SEI layer during Li deposition/stripping. The uneven surface reflects a mossy structure typical of lithium dendrite formation. Electrolytes with TCP-S_8 polymers, in contrast, exhibit a more uniform SEI morphology that does not contain surface defects after cycling (Figure 2-2b). The morphology consists mostly of particle-like structures, likely from the organic and inorganic polysulfides/sulfides. EDS (Figure 2-2c) illustrates that sulfur is evenly distributed across the SEI

Figure 2-2. (a,b) Environmental scanning electron microscopy (ESEM) images of the SEI built up on stainless steel after 50 cycles with no polymer additive (a) and a TCP-S_8 additive (b). (c) Energy-dispersive X-ray spectroscopy (EDS) illustrating the distribution of sulfur in the SEI with the TCP-S_8 additive. (d,e) The morphology of lithium metal after 50 cycles with no polymer additive (d) and a TCP-S_8 additive (e). The deposition capacity was 1 mAh g^{-1} and the current was 2 mA g^{-1}.

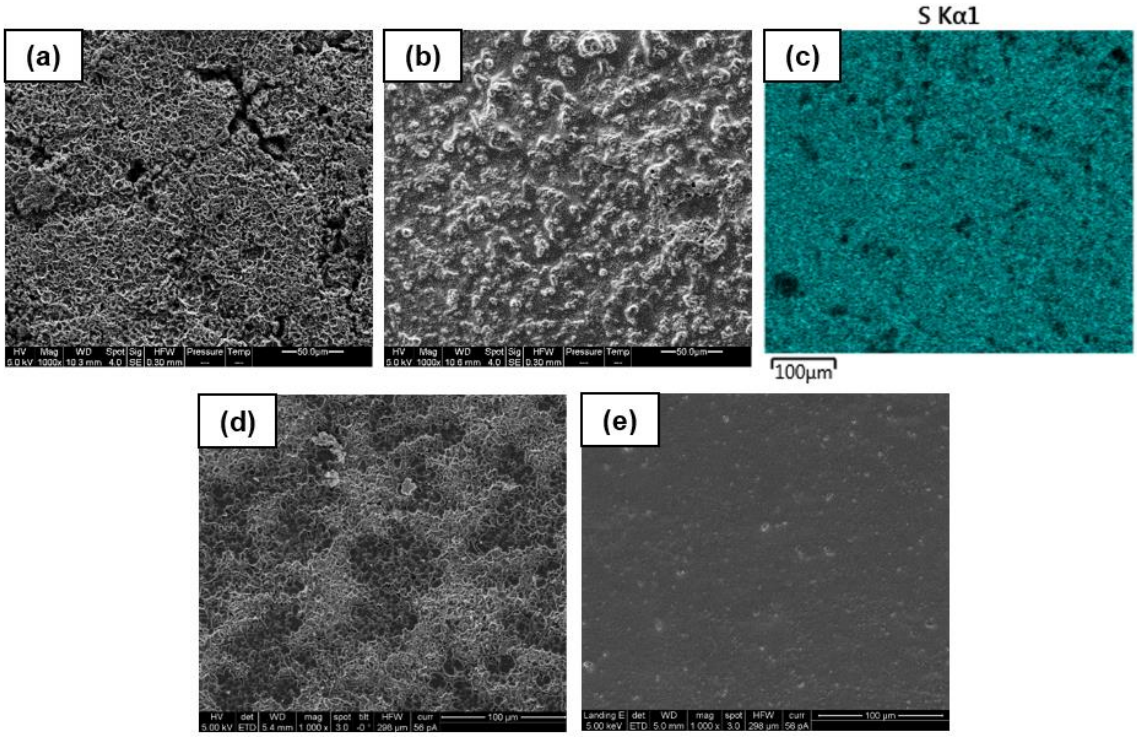

despite TCP-S_8 being insoluble in the electrolyte. The even distribution of sulfur throughout the SEI layer suggests that upon Li deposition/stripping, the organic and inorganic polysulfides dissolve into the electrolyte and co-deposit to form the hybrid SEI layer.[26] Owing to the stable hybrid SEI layer, a uniform and dendrite-free Li metal is achieved (Figure 2-2e). In contrast, the dendrite morphology from the control sample is readily apparent on the Li metal surface (Figure 2-2d).

The chemical components of the control and hybrid SEI layer were studied using XPS, specifically focusing on the composition of the surface layer (Figure 2-3). Peaks at 167.2, 168.7, and 170.0 eV in the S 2*p* XPS spectra both with and without the polymer additive (Figure 2-3a and 2-3c) represent the decomposition of LiTFSI.[22] When TCP-S_8 was added into the electrolyte, additional peaks at 159.9 and 161.3 eV appear, corresponding to Li_2S and Li_2S_2, respectively.

Figure 2-3. S 2*p* (a,c) and C 1*s* (b,d) x-ray photoemission spectroscopy (XPS) of the solid-electrolyte interface formed on stainless steel after 100 cycles using the control electrolyte (a, b) and with a TCP-S_8 additive (c, d).

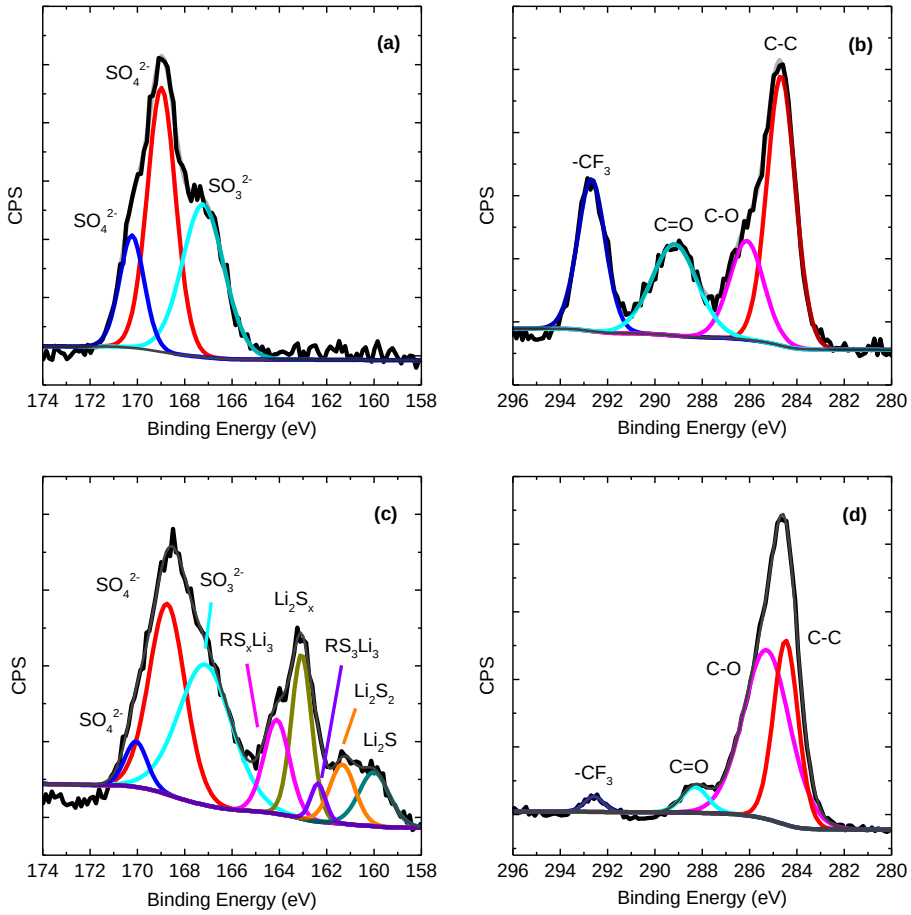

Lithium polysulfides, products of both polymer decomposition and disproportionation, appear in the S 2*p* spectrum at 163.0 eV. Organic polysulfides are also detected in the SEI layer with peaks at 162.4 eV and 164.0 eV (RS_3Li_3 and RS_xLi_3, respectively). The presence of inorganic Li sulfides and organopolysulfides in the SEI layer improve its stability and flexibility, as evidenced by the stable SEI structure after Li deposition/stripping (Figure 2-2b). Additionally, the C 1*s* spectrum for the TCP-S_8 additive shows a significantly reduced $–CF_3$ peak compared to the control sample (Figure 2-3c and 2-3d). This reduced peak relates to the suppressed decomposition rate of LiTFSI when using the sulfur polymer, which is consistent with previous studies on SEI formation with long-chain lithium polysulfides and comparable organosulfide polymers.[11]

Electrochemical performance

The dendrite-free deposition of Li metal and formation stable hybrid SEI layers enabled by the TCP-S_x polymers effectively improve the cycling performance of Li deposition/stripping. The polymers containing various sulfur contents were used as additives. The CE of Li deposition/stripping was studied in coin cells with a stainless steel electrode and lithium metal counter electrode. When depositing 1 mAh cm^{-2} of lithium at a current density of 2 mA cm^{-2}, the control sample with only $LiNO_3$ additive demonstrated a steep drop in deposition efficiency around 175 cycles. Adding TCP-S_2 does not extend the cycling life significantly, but does maintain the deposition efficiency of the control sample on a cycle-by-cycle basis. This is because that no inorganic Li sulfide is produced by breaking the disulfide bond, only organosulfides. Although these organosulfides are beneficial for the improvement of flexibility, the inorganic Li sulfides are necessary to provide mechanical stiffness to the SEI layers.[26] Increasing the sulfur order of the TCP polymers can ensure the generation of both inorganic Li sulfides and organosulfides, with these species synergistically enhancing the cycling stability of Li deposition/tripping. As shown in Figure 2-4a, stable deposition was observed with both the TCP-S_5 and TCP-S_8 additives, averaging 96.7% and 97.3% lithium deposition efficiency over 350 cycles, respectively. The lithium deposition efficiency did not drop below 90% until after 400 cycles with the TCP-S_8 additive. Comparably, samples with elemental sulfur employed as an additive, which can only generate inorganic Li sulfides, dropped below 90% CE after 300 cycles. This demonstrates how organosulfides provide flexibility to the SEI and, in turn, prolong the cycling life of Li deposition/stripping.

The voltage hysteresis between deposition and stripping also highlights the stability of SEI formation with TCP-S_x polymers (Figure 2-4b). The end-of-life profile essentially mirrors that of the deposition profile – a large spike in the voltage hysteresis corresponds to sharp decreases in

lithium deposition efficiency. The $TCP\text{-}S_8$ additive had the lowest voltage hysteresis throughout the cycle life of the control and sulfur additive samples. Most notably, the hysteresis was approximately 100 mV lower throughout all cycling compared to using $Li_2S_8/LiNO_3$, suggesting that the polymer improves the ionic conductivity of the SEI more than inorganic polysulfides.[22] Cells with an elemental sulfur additive had a similar initial hysteresis profile, but also exhibited a spike between 25 and 50 cycles, possibly related to the breakdown of sulfur to inorganic sulfides. The $TCP\text{-}S_x$ polymer additives showed a flat profile both initially and throughout 300+ cycles, confirming the significance of the organic/inorganic hybrid SEI layer in preventing lithium dendrites.

Figure 2-4. (a) Lithium deposition efficiency of cells with the control electrolyte, $TCP\text{-}S_x$ polymers, and sulfur additives. The cells were cycled to a capacity of 1 mAh cm^{-2} at a current rate of 2 mA cm^{-2}. (b) The voltage hysteresis from lithium deposition and stripping.

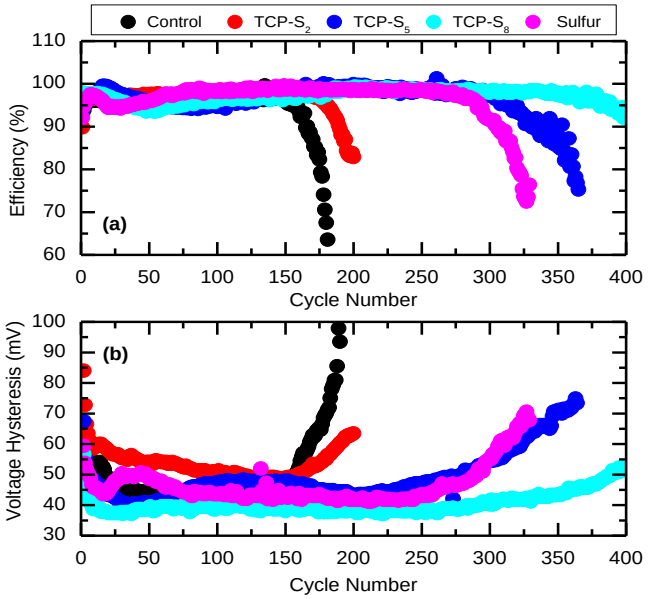

Conclusion

Polysulfides have previously been shown to suppress dendrite growth, but contribute to a low electrolyteionic conductivity and, therefore, a high voltage hysteresis during repeated lithium deposition and stripping. $TCP\text{-}S_x$ polymers created a continuous SEI layer through the formation of both organic and inorganic polysulfides. The TCP-based polymer with the highest sulfur content, $TCP\text{-}S_8$ (83.7 wt% sulfur), demonstrated the most stable SEI with a 97.3% average Coulombic efficiency over 350 cycles and >90% efficiency through 400 cycles at a current density of 2 mA

cm^{-2} and a deposition capacity of 1 mAh cm^{-2}. TCP-S_8 also lowered the average voltage hysteresis by 100 mV compared to using only inorganic polysulfides. Between the facile synthesis technique of the sulfur-rich polymer and the impressive morphological and electrochemical performance, this study offers promising insights to properly engineer SEI layers on lithium metal to meet the growing demand for energy storage.

References

[1] J. M. Tarascon, M. Armand, *Nature* **2001**, *414*, 359.

[2] M. A. Kiani, M. F. Mousavi, M. S. Rahmanifar, *Int. J. Electrochem. Sci.* **2011**, *6*, 2581.

[3] P. Bruce, S. Freunberger, *Nat. Mater.* **2012**, *11*, 19.

[4] J. B. Goodenough, Y. Kim, *Chem. Mater.* **2010**, *22*, 587.

[5] R. Cao, W. Xu, D. Lv, J. Xiao, J. Zhang, *Adv. Energy Mater.* **2015**, *5*, 1.

[6] X. B. Cheng, R. Zhang, C. Z. Zhao, F. Wei, J. G. Zhang, Q. Zhang, *Adv. Sci.* **2015**, *3*, 1.

[7] S. Zhang, K. Ueno, K. Dokko, M. Watanabe, *Adv. Energy Mater.* **2015**, *5*, 1.

[8] L. Fan, H. L. Zhuang, L. Gao, Y. Lu, L. A. Archer, *J. Mater. Chem. A* **2017**, *5*, 3483.

[9] L. Chen, J. G. Connell, A. Nie, Z. Huang, K. R. Zavadil, K. C. Klavetter, Y. Yuan, R. Shahbazian-yassar, J. A. Libera, U. Mane, W. Elam, *J. Mater. Chem. A* **2017**, *5*, 12297.

[10] G. A. Umeda, E. Menke, M. Richard, K. L. Stamm, F. Wudl, B. Dunn, *J. Mater. Chem.* **2011**, *21*, 1593.

[11] Y. Liu, D. Lin, Z. Liang, J. Zhao, K. Yan, Y. Cui, *Nat. Commun.* **2016**, *7*, 10992.

[12] J. Zheng, M. H. Engelhard, D. Mei, S. Jiao, B. J. Polzin, J.-G. Zhang, W. Xu, *Nat. Energy* **2017**, *2*, 17012.

[13] X. Q. Zhang, X. B. Cheng, X. Chen, C. Yan, Q. Zhang, *Adv. Funct. Mater.* **2017**, *27*, 1.

[14] Q. Zhang, J. Pan, P. Lu, Z. Liu, M. W. Verbrugge, B. W. Sheldon, Y. T. Cheng, Y. Qi, X. Xiao, *Nano Lett.* **2016**, *16*, 2011.

[15] H. Ota, K. Shima, M. Ue, J. Yamaki, *Electrochim. Acta* **2004**, *49*, 565.

[16] F. Ding, W. Xu, G. L. Graff, J. Zhang, M. L. Sushko, X. Chen, Y. Shao, M. H. Engelhard, Z. Nie, J. Xiao, X. Liu, P. V Sushko, J. Liu, J. G. Zhang, *J. Am. Chem. Soc.* **2013**, *135*, 4450.

[17] Y. V. Mikhaylik, J. R. Akridge, *J. Electrochem. Soc.* **2004**, *151*, A1969.

[18] H. Kim, G. Jeong, Y.-U. Kim, J.-H. Kim, C.-M. Park, H.-J. Sohn, *Chem. Soc. Rev.* **2013**, *42*, 9011.

[19] W. Xu, J. Wang, F. Ding, X. Chen, E. Nasybulin, Y. Zhang, J.-G. Zhang, *Energy Environ. Sci.* **2014**, *7*, 513.

[20] Y. V Mikhaylik, *U.S. Patent 7,358,012* **2008**.

[21] D. Aurbach, E. Pollak, R. Elazari, G. Salitra, C. S. Kelley, J. Affinito, *J. Electrochem. Soc.* **2009**, *156*, A694.

[22] W. Li, H. Yao, K. Yan, G. Zheng, Z. Liang, Y.-M. Chiang, Y. Cui, Nat. Commun. **2015**, 6, 7436.

[23] C. Yan, X. B. Cheng, C. Z. Zhao, J. Q. Huang, S. T. Yang, Q. Zhang, *J. Power Sources* **2016**, *327*, 212.

[24] S. Chen, F. Dai, M. L. Gordin, Z. Yu, Y. Gao, J. Song, D. Wang, *Angew. Chemie - Int. Ed.* **2016**, *55*, 4231.

[25] S. Chen, Y. Gao, Z. Yu, M. L. Gordin, J. Song, D. Wang, *Nano Energy* **2017**, *31*, 418.

[26] G. Li, Y. Gao, X. He, Q. Huang, S. Chen, S. H. Kim, D. Wang, *Nat. Commun.* **2017**, *8*, 1.

[27] W. J. Chung, J. J. Griebel, E. T. Kim, H. Yoon, A. G. Simmonds, H. J. Ji, P. T. Dirlam, R. S. Glass, J. J. Wie, N. a Nguyen, B. W. Guralnick, J. Park, A. Somogyi, P. Theato, M. E. Mackay, Y.-E. Sung, K. Char, J. Pyun, *Nat. Chem.* **2013**, *5*, 518.

[28] Z. Sun, M. Xiao, S. Wang, D. Han, S. Song, G. Chen, Y. Meng, *J. Mater. Chem. A* **2014**, *2*, 9280.

[29] Y. Zhang, Y. Peng, Y. Wang, J. Li, H. Li, J. Zeng, J. Wang, B. J. Hwang, J. Zhao, *Sci. Rep.* **2017**, *7*, 11386.

[30] C. Zu, N. Azimi, Z. Zhang, A. Manthiram, *J. Mater. Chem. A* **2015**, *3*, 14864.

[31] L. Ma, M. S. Kim, L. A. Archer, *Chem. Mater.* **2017**, *29*, 4181.

[32] L. Suo, Y.-S. Hu, H. Li, M. Armand, L. Chen, *Nat. Commun.* **2013**, *4*, 1481.

[33] J. Qian, W. A. Henderson, W. Xu, P. Bhattacharya, M. Engelhard, O. Borodin, J.-G. Zhang, *Nat. Commun.* **2015**, *6*, 6362.

[34] L. Carbone, M. Gobet, J. Peng, M. Devany, B. Scrosati, S. Greenbaum, J. Hassoun, *ACS Appl. Mater. Interfaces* **2015**, *7*, 13859.

[35] Q. Ma, Z. Fang, P. Liu, J. Ma, X. Qi, W. Feng, J. Nie, Y. S. Hu, H. Li, X. Huang, L. Chen, Z. Zhou, *ChemElectroChem* **2016**, *3*, 531.

[36] J. Lim, U. Jung, W. T. Joe, E. T. Kim, J. Pyun, K. Char, *Macromol. Rapid Commun.* **2015**, *36*, 1103.

[37] C. Barchasz, F. Molton, C. Duboc, J. C. Lepretre, S. Patoux, F. Alloin, *Anal Chem* **2012**, *84*, 3973.

[38] A. B. D. Nandiyanto, M. A. Fadhlulloh, T. Rahman, A. Mudzakir, *IOP Conf. Ser. Mater. Sci. Eng.* **2016**, *128*.

[39] G. A. Voyiatzis, K. S. Andrikopoulos, G. N. Papatheodorou, E. I. Kamitsos, G. D. Chryssikos, J. A. Kapoutsis, S. H. Anastasiadis, G. Fytas, *Macromolecules* **2000**, *33*, 5613.

[40] R. Miao, J. Yang, Z. Xu, J. Wang, Y. Nuli, L. Sun, *Sci. Rep.* **2016**, *6*, 21771.

Chapter 3

A synergistic lithium metal anode solid-electrolyte interface with carbon tetrachloride and lithium nitrate additives

Abstract

The intercalation chemistry utilized by graphite anodes in state-of-the-art lithium-ion batteries (LIBs) has enabled the commercialization of numerous consumer electronic devices. Unfortunately, the relatively low specific capacity and energy density of graphite stymies the economic impact of LIBs. A shift to lithium metal anodes could greatly improve the efficiency of transportation and electricity generation systems by enabling new battery chemistries such as lithium-sulfur. Lithium metal possesses many promising electrochemical properties, but, because it is so chemically reactive, attention must be paid to engineering uniform surface films at the solid-electrolyte interface (SEI) that promote fast Li^+ diffusion. Halogenated electrolyte additives accomplish this by depositing lithium halide salts into the SEI to increasing the potential gradient between the electrode surface and the bulk electrolyte. Carbon tetrachloride, a common halogenated solvent, reacts with both N_xO_y groups and carbonates to form lithium chloride and a polymer. The hybrid SEI layer promotes stable lithium deposition for over 350 cycles, with an average coulombic efficiency > 98%. Improved electrochemical performance was also demonstrated at a high deposition capacity (4 mAh cm^{-2}).

Introduction

Lithium-ion batteries (LIBs) have been a remarkably successful technology since their commercialization by Sony in 1991, enabling the creation of portable electronic devices and electric vehicles.[1]-[3] State-of-the-art LIBs typically rely on intercalation chemistry, whereby the Li^+ ion reversibly inserts between the stacked layers of a transition metal oxide cathode and a graphite anode. Cells with these electrode components achieve a cell voltage $\sim$ 4V, but their low specific capacity caps their energy density at around 400 Wh kg^{-1}.[4]-[5] Additionally, the high cost of transition metal oxides caps the economic impact of intercalation-dependent LIBs.[6]-[7]

Lithium-sulfur (Li-S) batteries have long been considered to be the next major leap in battery performance. In contrast to LIBs, Li-S batteries rely on conversion chemistry, whereby sulfur cathodes react with Li^+ ions from lithium metal anodes. As a cathode material, sulfur possesses some enticing attributes, namely a high specific capacity (1675 mAh g^{-1}) and a low cost due to its high natural abundance.[4]-[8] As an anode material, lithium metal offers an electrochemical capacity nearly 10 times higher than that of graphite, low mass to achieve a high gravimetric energy density, and a low density to achieve a high volumetric energy density.[9]-[11]

The promise of cheap, energy dense Li-S batteries has tantalized researchers for decades, but a true breakthrough remains elusive owing to some of the fundamental scientific properties of the proposed electrode components. The issues associated with sulfur cathodes are well-documented: low electrical conductivity of the active materials, the polysulfide shuttle effect, lithium sulfide (Li_2S and Li_2S_2) deposition on the electrodes, and volume expansion upon lithiation.[4].[12]-[13] Many researchers have attempted to solve these issues by engineering frameworks to confine sulfur-containing species to the cathode.[14]-[17] While offering some progress, more attention also must be paid to how sulfur-containing species react with lithium metal. Lithium possesses the lowest electrochemical potential of any substance; therefore, it readily

decomposes many Li-S battery compatible materials, especially liquid electrolytes.[10] These decomposed components form a solid-electrolyte interface (SEI). In order for the SEI to be beneficial to battery performance, it must enable uniform lithium deposition during the course of cycling. Without controlled deposition, potential gradients across the SEI will cause concentrations of lithium metal to steadily build up in the passivation film, forming structures known as "dendrites", characterized by their long, branch-like structures.[18]-[20] Over the course of cycling, these dendrites can penetrate the separator and short-circuit the battery. Unfortunately, polysulfide-rich electrolytes corrode lithium metal, guaranteeing an uneven distribution of charge of the electrode and dendrite formation/growth.

The goal, then becomes to identify molecules and materials that enable a slow-growing, uniform SEI morphology. One of the most effective additives studied to date is lithium nitrate ($LiNO_3$), which has become ubiquitous in Li-S batteries.[21] The stable passivation film formed with $LiNO_3$ not only improves Li-ion diffusivity, but also mitigates the parasitic polysulfide shuttle effect. Rather than forming insulating lithium sulfide, $LiNO_3$ works in conjuction with polysulfides to form a surface film rich in LiN_xO_y and LiS_xO_y species that can also limit the decomposition rate of the ionically conductive lithium salt.[22] Because $LiNO_3$ irreversibly decomposes in this SEI formation process, though, polysulfides will corrode the lithium metal anode once all of the $LiNO_3$ is consumed.[23]-[24] Since $LiNO_3$ demonstrated synergistic behavior with polysulfides, it stands to reason that $LiNO_3$ can also provide beneficial SEI formation properties with other additives.

Halogenated materials are one type of additive that have proven to provide lithium metal protection in both carbonate- and ether-based electrolyte systems. Density functional theory studies have shown that halides reduce the activation barrier for Li diffusion; therefore, passivation films have been engineered both with halides directly added into the electrolyte or through decomposition reactions of halogenated salts.[25] Archer *et al.* took that observation from the DFT studies and experimentally demonstrated that lithium fluoride (LiF) is a key component responsible for

stabilizing the SEI and improving the columbic efficiency of lithium electrodeposition. The insulating property of LiF establishes a potential gradient between the lithium metal surface and the bulk electrode, a gradient that drives Li-ion diffusion.[26]-[29] LiF is a well-known decomposition product of lithium salts such as $LiPF_6$ and LiTFSI [22], [30], which sparked the engineering of additional electrolyte components to optimize the amount of LiF that would be formed at the lithium metal/electrolyte interface, including fluoroethlyene carbonate (FEC) [31], bis(2,2,2-trifluoroethyl) ether (BTFE) [32], 1,1,2,2-tetrafluoroethyl-2,2,3,3-tetrafluoropropyl ether (TTE) [33], and Freon R134a.[27]

Other halides have been relatively ignored despite possessing similar chemical properties to their fluorinated counterparts. Lithium chloride (LiCl), lithium bromide (LiBr), and lithium iodide (LiI) all provide the same insulating properties that can drive Li diffusion. Chlorosilanes, studied by Wudl *et al.*, prevent gas phase reactions at the lithium metal surface by forming a protection layer primarily consisting of lithium chloride (LiCl) and silicon-based byproducts.[34] Trimethylsilyl chloride was shown by Chowdari *et al*. to convert both lithium hydroxide (LiOH) and lithium oxide (Li_2O) into the more functional LiCl.[35] Nazar *et al.* demonstrated how the simple reduction reaction of metal chlorides (MCl_x, where M = In, Zn, Bi, As) on lithium metal produces both LiCl and Li_yM_z alloys. *Operando* optical microscopy illustrated how the alloy/LiCl composite SEI prevented lithium metal aggregation and nucleation and enabled a smooth surface morphology.[36] Archer *et al.* crosslinked silicon tetrachloride ($SiCl_4$) with propylene carbonate (PC) to form a carbonate oligomer doped with lithium chloride. Lithium metal catalyzed the ring-opening of PC that enabled the formation of the oligomer. Yushin *et al.* showed how both LiBr and LiI limit Li_2S deposition.[37] The Br^- and I^- anions react with the organic electrolyte component 1,2-dimethoxyethane (DME) to form hydrobromic/hydroiodic acid (HBR/HI) and a DME-oligomer.[38]-[39] Archer *et al*. reported that the strong Lewis acid AlI_3 could decompose into LiI and a Li_xAl alloy *via* a mechanism similar to the one demonstrated by Nazar *et al.* Without other

additves, the LiI/Li_xAl protection layer achieved a stable coulombic efficiency of ~95% over 100 cycles in lithium metal/stainless steel cells.[40]

Given the effectiveness of both $LiNO_3$ and halogenated materials for providing lithium metal protection, further advances could be had by combining these materials into a single electrolyte. One of the drawbacks to using any of the additives discussed above as the sole source of lithium protection is that they are depleted during the course of cycling. Combining two or more of these types of additives could slow the depletion rate of each individual component by creating a competitive, yet synergistic reaction environment. In this study, $LiNO_3$ and a highly chlorinated solvent, carbon tetrachloride (CCl_4), were chosen to evaluate whether such an environment could be achieved. CCl_4 is a very stable solvent, but can react with the electrolyte decomposition products in a manner similar to the mechanism described by Archer *et al.*[37] An ether electrolyte, typically used in Li-S batteries, with an optimized amount of CCl_4 was able to achieve a lithium an average deposition efficiency of greater than 98% for 350 cycles, more than two times as many cycles compared to only using $LiNO_3$. Characterization of the surface films illustrated that this improved performance could be attributed to the formation of a hybrid lithium metal surface film consisting of LiCl and a polymer from the reaction of CCl_4 with nitrates and carbonates. This unique surface film suppressed lithium dendrite formation.

Experimental Methods

Electrolyte preparation

Carbon tetrachloride (≥99.5%, Sigma-Aldrich) was added in varying amounts to an electrolyte of 1M lithium bis(trifluoromethanesulfonyl)imide (LiTFSI, BASF) in 1:1v 1,3-dioxolane (DOL, BASF) and 1,2-dimethoxyethane (DME, BASF) with 4 wt% lithium nitrate

($LiNO_3$, 99.99% trace metals basis, Sigma-Aldrich). The electrolyte was prepared in an MBraun argon-filled glove box with H_2O and O_2 less than 1 ppm. Other chlorinated hydrocarbon additives were also studied and were prepared in the same manner (Supplemental Information and Supplemental Figure B-1).

Materials characterization

To characterize the solid-electrolyte interface that formed on the stainless steel electrode and the changes to the properties of lithium metal, X-ray photoemission spectroscopy (XPS) and field emission scanning electron microscopy (FESEM) were conducted. XPS spectra were collected on a PHI *VersaProbe* II Scanning XPS Microprobe. The binding energies were calibrated using the C1s peak at 284.7 eV. FESEM was run on an FEI Nova NanoSEM 630 to determine the morphology of the solid-electrolyte interface formed on stainless steel and lithium metal from lithium deposition and stripping. The electrodes were rinsed with DOL to remove residual electrolyte components. Air-tight containers were used to transfer the electrodes to each piece of characterization equipment.

Electrochemical performance

CR2016 coin cells were assembled in an argon-filled glove box with stainless steel and lithium metal electrodes using Neware battery testers. Lithium metal deposition and stripping was done at a constant current rate at room temperature. Time was used to control the deposition capacity. Stripping was completed when the voltage reached 0.5V vs. Li/Li^+.

Results and Discussion

The two-electrode configuration where lithium is plated and stripped from stainless steel has been shown to provide an accurate representation of the SEI under normal battery conditions. Importantly, characterizing the surface film on the stainless steel also negates interface that often occurs when studying films on lithium metal. All *ex-situ* characterization on the SEI, therefore, was conducted with the SEI grown on the stainless steel electrode. The change in the morphology of the lithium metal surface during cycling was also studied.

SEIs formed in ether electrolytes with a $LiNO_3$ additive contain a variety of lithiated components. Figure 3-1 shows the XPS spectra of the SEI films with $LiNO_3$ grown on stainless steel after 25 cycles (i.e., after lithium metal was deposited and stripped from stainless steel 25 times). Li_xNO_y forms directly from $LiNO_3$ reduction, while $LiNO_3$ can also form LiOR and RCOOLi species in concert with DOL. The most intense peaks, at 399.5 eV and 397.6 eV, in the N1s spectrum are associated with the decomposition of LiTFSI, corresponding to $Li_2NSO_2CF_3$ and Li_3N, respectively. The less intense peaks are still notable, corresponding to NO_2^- (404.3 eV) and NO_3^- (407.6 eV), with $LiNO_2$ being a known reduction product of $LiNO_3$. Moving to the O1s spectrum, peaks below 530 eV are typically assigned to Li-O species, i.e. LiOH. Carbonates, Li_2CO_3, manifest in both the O1s spectrum at 531.5 eV, though appear to be a minor component of the SEI. Li_3N and LiOH also appear in the Li1s spectrum at 54.3eV and 54.9 eV, respectively. Finally, given that there are no chlorinated components in the control sample, there are no signals from the Cl2p spectrum.

Figure 3-1. X-ray photoemission spectroscopy (XPS) of the solid electrolyte interface formed on stainless steel after 25 cycles with an electrolyte containing 4wt% $LiNO_3$. a) N1s, b) O1s, c) Li1s, and d) Cl2p.

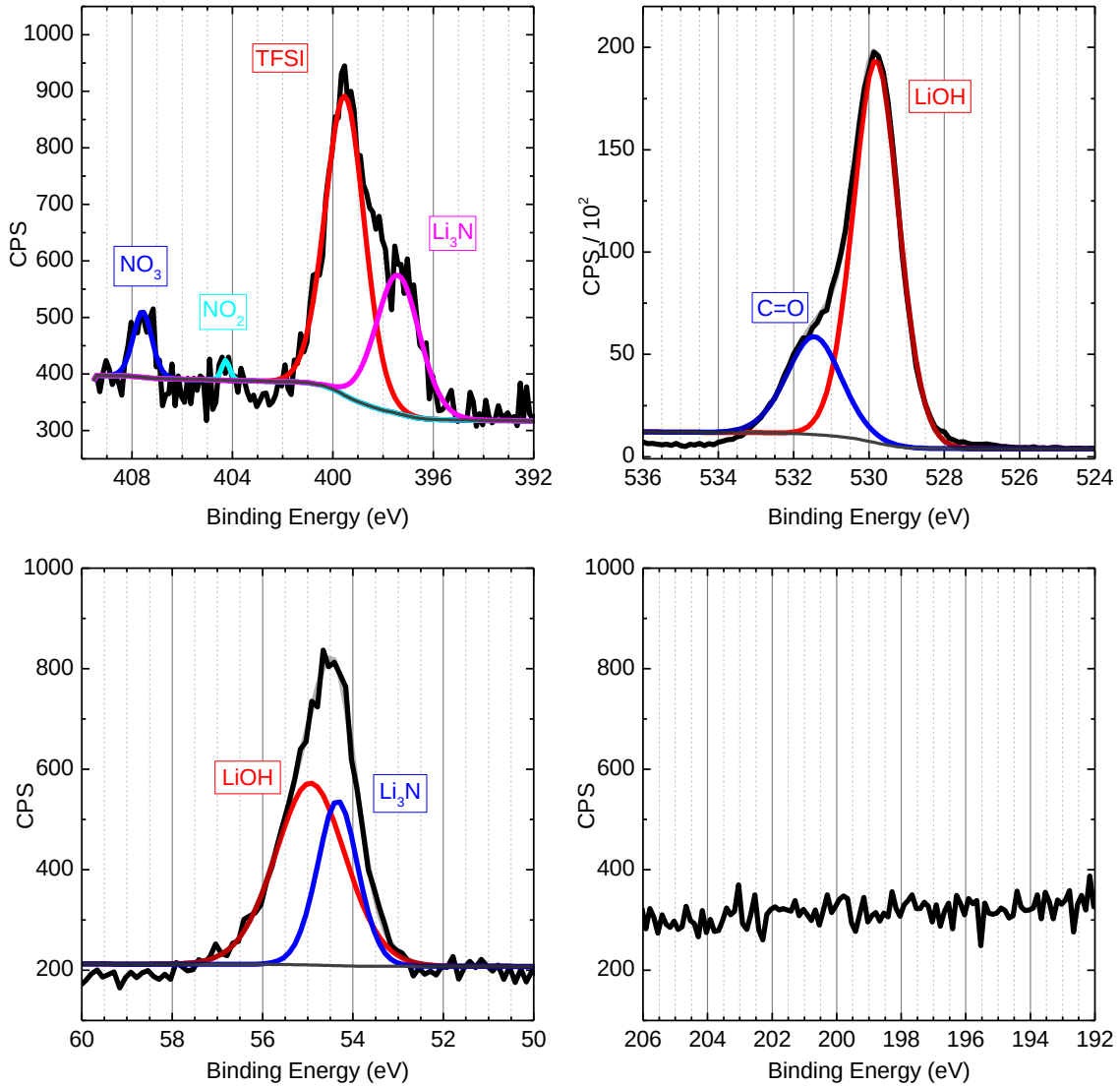

The chemical environment of the SEI is altered significantly with the addition of CCl_4 to the electrolyte, as shown by XPS in (Figure 3-2), taken under the same conditions as the control sample. In the N1s spectrum, the peak at 398.9 eV corresponds to the formation of N-O bonds, in contrast to the Li_3N peak from the control sample. Similarly, the O1s peak associated with LiOH is not present; rather, a peak at 532.8 eV corresponds to C-O bonds. The Li_2CO_3 peak shares similar intensity to the C-O peak, a contrast to the ratio of the Li_2CO_3/LIOH intensities in the control sample. The L1s spectrum further confirms that lack of Li_3N and LiOH. The new peak in this

Figure 3-2. X-ray photoemission spectroscopy (XPS) of the solid electrolyte interface formed on stainless steel after 25 cycles with an electrolyte containing both 50mM CCl_4 and 4wt% $LiNO_3$. a) N1s, b) O1s, c) Li1s, and d) Cl2p.

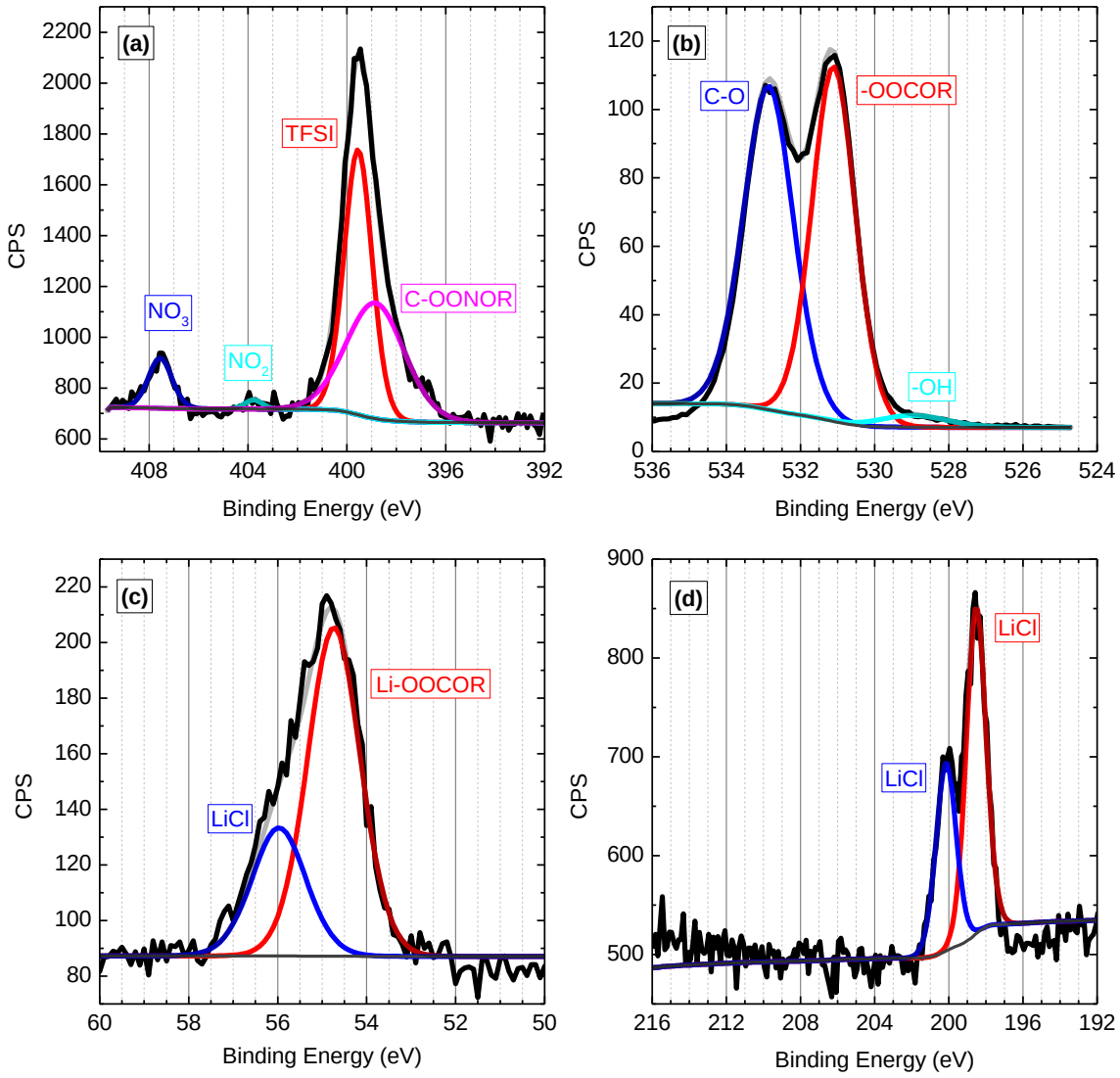

spectrum at 56.0 eV corresponds to LiCl. The formation of Cl^- is confirmed by the two peaks in the Cl2p spectrum, particularly that one these peaks are below 200 eV (198.6 eV), a signature of forming inorganic chlorides.[36] The spectra suggests that CCl_4 reacts with both nitrates and carbonates *via* a similar mechanism described by Archer *et al.*, in which silicon tetrachloride ($SiCl_4$) acted as a cross-linking agent in the presence of ring-opened propylene carbonate.[37]

Scanning electron microscopy (SEM) was used to illustrate how these changes in the surface chemistry impact the morphology of the SEI. Figure 3-3 shows the top view of the SEIs of

Figure 3-3. Top view field emission scanning electron microscopy (FESEM) images of the SEI on stainless steel (a, b) and lithium metal (c, d) with the control electrolyte (a, c) and 50mM CCl_4 added electrolyte (b, d).

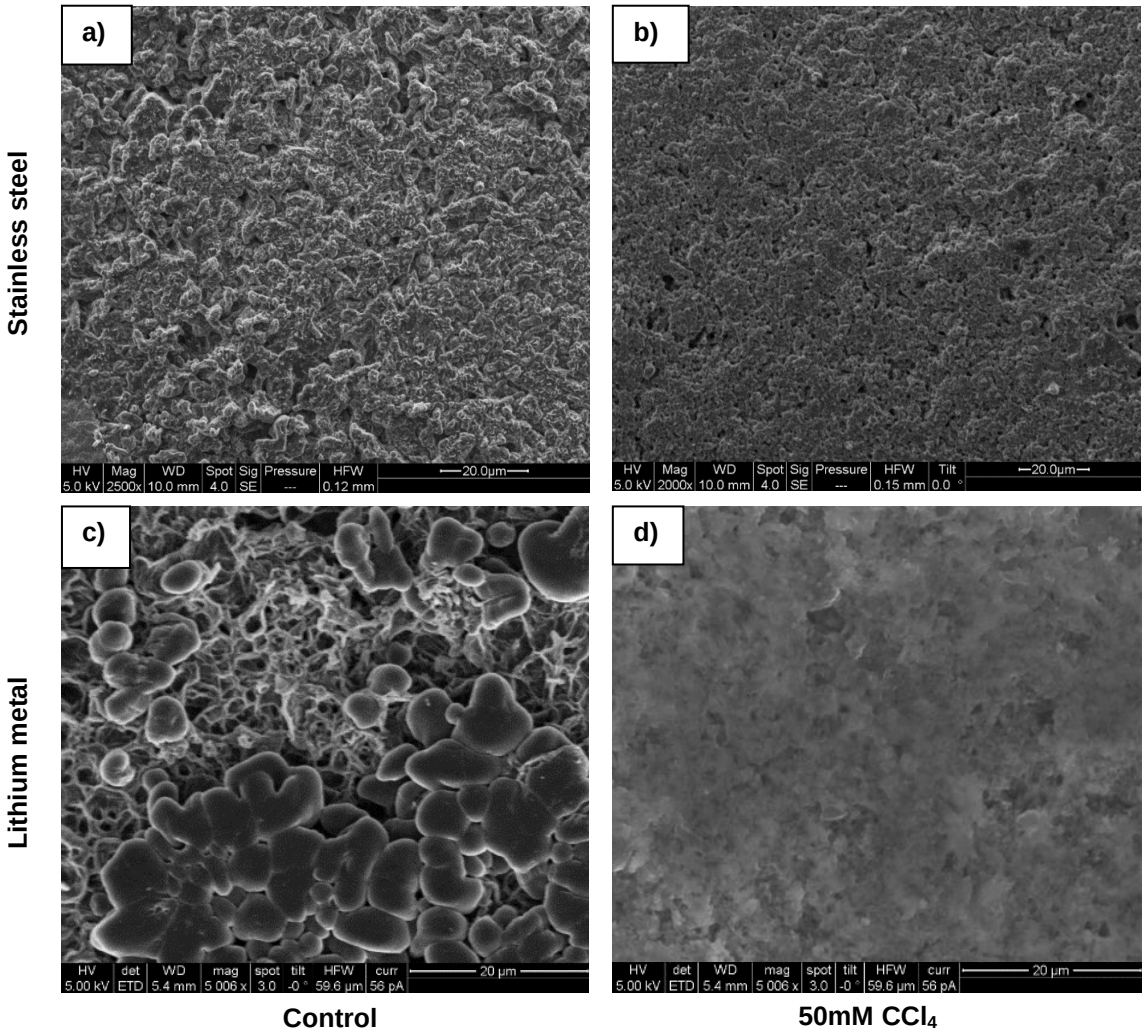

the control and CCl_4-containing electrolytes grown on stainless steel. A 1 mAh/cm^2 capacity of lithium was deposited on stainless steel in each cycle at a current rate of 2 mA/cm^2. As has been shown in previous studies, electrolytes only using $LiNO_3$ form an uneven, mossy passivation film, which was observed in this study as well. In contrast, SEIs with CCl_4 demonstrate a smooth morphology, with no noticeable dendrite formation. The reduction of CCl_4 to LiCl provides an insulating component that, when properly optimized, increases the Li^+ potential gradient and, therefore, increases the Li^+ diffusion rate through the more ionically conductive parts of the SEI. A schematic of the reaction between CCl_4 and $LiNO_3$ to form an organic/inorganic hybrid SEI and its

Figure 3-4. The reaction between carbon tetrachloride and lithium nitrate to form an organic polymer and lithium chloride, which work together to suppress lithium dendrite formation and enable a uniform SEI layer.

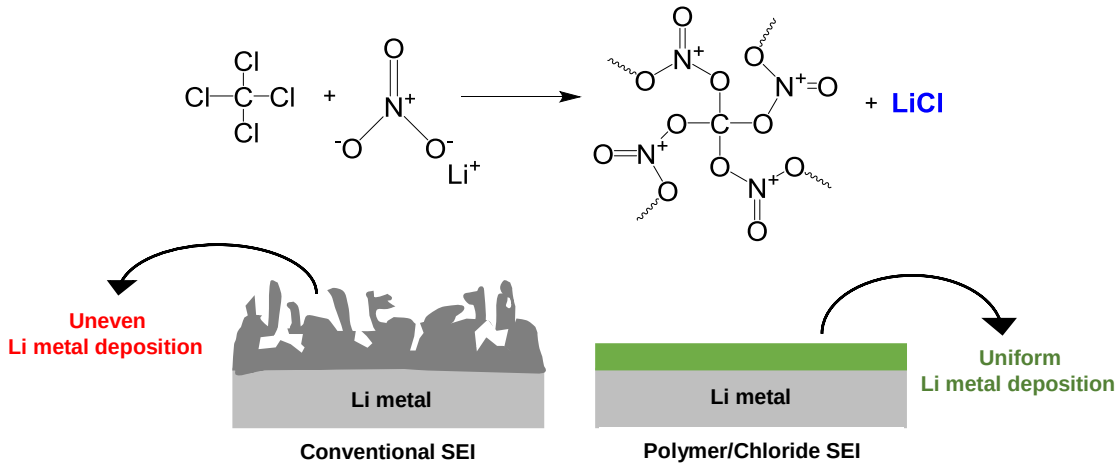

effect on the morphology of the SEI is illustrated in Figure 3-4. Fast Li^+ diffusion rate ensures a uniform charge distribution throughout the SEI and lowers the likelihood of forming dendrites.[27], [30], [37]

The electrochemical stability of the SEI was characterized using a two-electrode configuration, whereby lithium was deposited and stripped on stainless steel. The effectiveness of the SEI was determined by calculating coulombic efficiency and voltage hysteresis. The coulombic efficiency is defined as the ratio of the capacity of lithium stripped from the stainless steel versus the capacity of lithium deposited on the surface; the voltage hysteresis is defined as the difference

Figure 3-5. The a) coulombic efficiency and b) voltage hysteresis profiles of Li/stainless steel cells with varying amount of CCl_4. A capacity of 1 mAh cm^{-2} lithium was deposited on stainless steel at a current rate of 2 mA cm^{-2}.

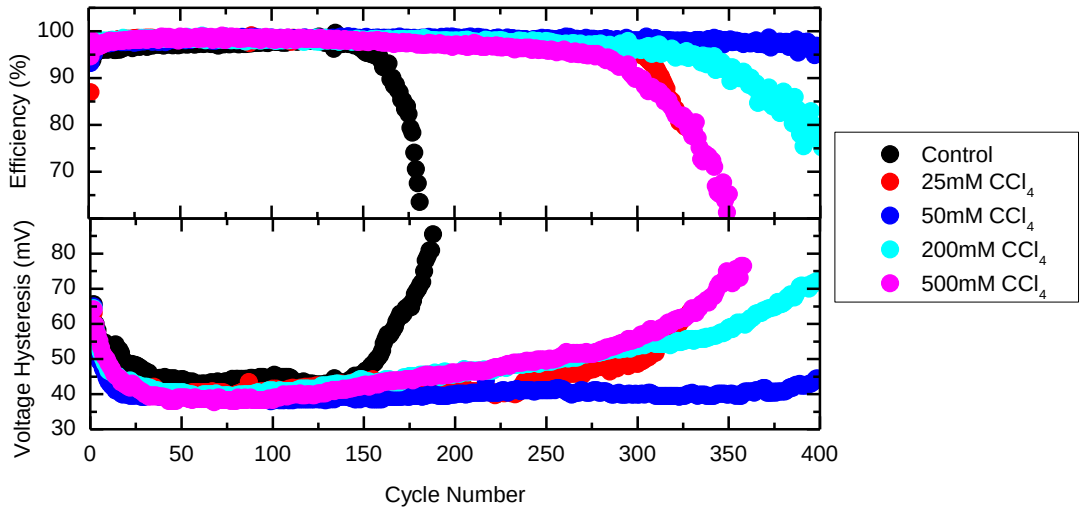

between the voltage upon deposition and the voltage upon stripping. The slope of the voltage profile is essentially flat for the entirety of deposition and stripping, so the voltage hysteresis can be readily determined at any capacity along this profile (Supplementary Figure B-2). Figure 3-5 shows both the coulombic efficiency and voltage hysteresis trends without CCl_4 and with various amount of CCl_4 at a deposition capacity of 1 mAh/cm^2 and a current of 2 mA/cm^2. Every sample containing CCl_4 exhibited better performance compared to the control sample, highlighting the importance that LiCl can play in SEI formation. The concentration of CCl_4 was optimized to 50mM, where an average columbic efficiency of 98.3% was achieved over the first 300 cycles and remained at above 90% for 400 cycles. Upon increasing beyond that concentration, the decrease in the ionic conductivity associated with forming LiCl outweighs the benefits of an increased potential gradient for Li^+ diffusion. This balance is especially clear in the voltage hysteresis profile, where the hysteresis continues to increase after around 100 cycles for the 200mM and 500mM samples. In

Figure 3-6. The coulombic efficiency and voltage hysteresis at a deposition capacity of 2 mAh cm^{-2} (a,b) and 4 mAh cm^{-2} (c,d) with the control and 50mM CCl_4 additive electrolytes.

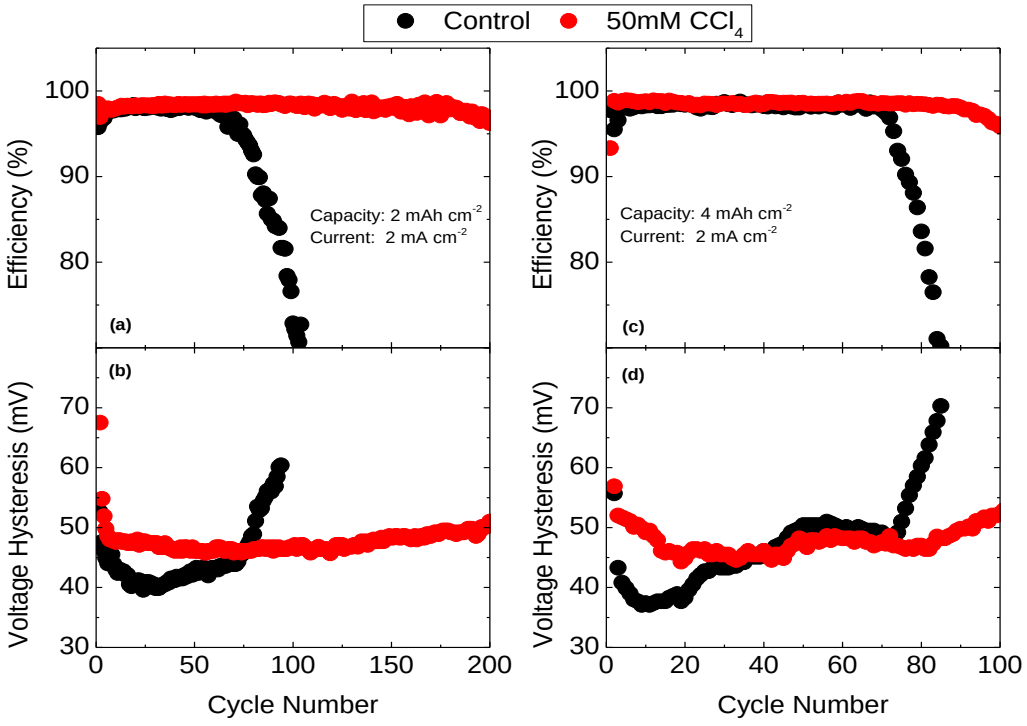

contrast, the properly tuned CCl_4 concentration demonstrates a stable voltage profile for around 375 cycles before resistance from the SEI begins to negatively impact the performance.

Improved SEI growth is also apparent at higher lithium deposition amounts (2 and 4 mAh/cm^2) (Figure 3-6). Under these more intense conditions, though, the voltage hysteresis for the CCl_4-containing electrolytes is actually greater than that of the control sample during initial SEI formation. At a higher deposition capacity, the surface area available for lithium deposition could be limited by the presence of CCl_4, which would result in the observed increase in voltage hysteresis. After many cycles, however, the benefits of LiCl appear to overtake any losses in surface area. The lithium deposition efficiency was also tested using with CCl_4 containing electrolytes without $LiNO_3$ (Supplementary Figure B-3). Even at the lowest deposition condition tested (1 mAh/cm^2), the coulombic efficiency failed to reach above 70%. Based on the XPS results, the benefits of CCl_4 in the electrolyte only manifest when it is able to react with $LiNO_3$ and its byproducts.

Conclusions

We demonstrated how lithium nitrate and carbon tetrachloride work together to form a stable solid electrolyte film to protect lithium metal anodes. The simple addition of carbon tetrachloride into the electrolyte causes reactions with both nitrates and carbonates to form a polymer and lithium chloride. These components ensure uniform lithium metal deposition that prevents dendrites. The hybrid SEI provides an insulating barrier that drives Li^+ diffusion from the electrode surface to the bulk electrolyte. The improved SEI layer exhibits stable cycling for 400 cycles in Li/stainless steel cells as well as improved performance at high deposition capacities (4 mAh cm^{-2}). In most studies, lithium nitrate is directly reduced on lithium metal to form a passivation film. This study offers a unique use for $LiNO_3$ that drive a new direction for

electrolyte additive synthesis and development, further facilitating the formation of surface species beneficial to smooth, uniform solid electrolyte interfaces on lithium metal.

References

[1] B. Dunn, H. Kamath, J.-M. Tarascon, *Science.* **2011**, *334*, 928.

[2] J. B. Goodenough, K.-S. Park, *J. Am. Chem. Soc.* **2013**, 135, 1167.

[3] G. E. Blomgren, *J. Electrochem. Soc.* **2017**, *164*, A5019.

[4] P. Bruce, S. Freunberger, *Nat. Mater.* **2012**, *11*, 19.

[5] J. W. Choi, D. Aurbach, *Nat. Rev. Mater.* **2016**, *1*, DOI 10.1038/natrevmats.2016.13.

[6] J. Cabana, L. Monconduit, D. Larcher, M. R. Palacín, *Adv. Mater.* **2010**, *22*, 170.

[7] M. A. Hannan, M. M. Hoque, A. Mohamed, A. Ayob, *Renew. Sustain. Energy Rev.* **2017**, *69*, 771.

[8] L. Chen, L. L. Shaw, *J. Power Sources* **2014**, *267*, 770.

[9] Y. Guo, H. Li, T. Zhai, *Adv. Mater.* **2017**, *29*, 1.

[10] D. Lin, Y. Liu, Y. Cui, *Nat. Nanotechnol.* **2017**, *12*, 194.

[11] R. Cao, W. Xu, D. Lv, J. Xiao, J. Zhang, *Adv. Energy Mater.* **2015**, *5*, 1.

[12] X. Ji, L. Nazar, *J. Mater. Chem.* **2010**, *20*, 9821.

[13] Y.-X. Yin, S. Xin, Y.-G. Guo, L.-J. Wan, *Angew. Chem. Int. Ed. Engl.* **2013**, *52*, 13186.

[14] R. Demir-Cakan, M. Morcrette, A. Guéguen, R. Dedryvère, J.-M. Tarascon, *Energy Environ. Sci.* **2013**, *6*, 176.

[15] X. Ji, K. T. Lee, L. F. Nazar, *Nat. Mater.* **2009**, *8*, 500.

[16] H. Chen, C. Wang, Y. Dai, S. Qiu, J. Yang, W. Lu, L. Chen, *Nano Lett.* **2015**, *15*, 5443.

[17] J. Song, M. L. Gordin, T. Xu, S. Chen, Z. Yu, H. Sohn, J. Lu, Y. Ren, Y. Duan, D. Wang, *Angew. Chemie - Int. Ed.* **2015**, *54*, 4325.

[18] Y. V. Mikhaylik, J. R. Akridge, *J. Electrochem. Soc.* **2004**, *151*, A1969.

[19] D. Wang, W. Zhang, W. Zheng, X. Cui, T. Rojo, *Adv. Sci.* **2017**, *4*, 1.

[20] X. B. Cheng, R. Zhang, C. Z. Zhao, F. Wei, J. G. Zhang, Q. Zhang, *Adv. Sci.* **2015**, *3*, 1.

[21] D. Aurbach, E. Pollak, R. Elazari, G. Salitra, C. S. Kelley, J. Affinito, *J. Electrochem. Soc.* **2009**, *156*, A694.

[22] W. Li, H. Yao, K. Yan, G. Zheng, Z. Liang, Y.-M. Chiang, Y. Cui, *Nat. Commun.* **2015**, *6*, 7436.

[23] C. Yan, X. B. Cheng, C. Z. Zhao, J. Q. Huang, S. T. Yang, Q. Zhang, *J. Power Sources* **2016**, *327*, 212.

[24] X. Liang, Q. Pang, I. R. Kochetkov, M. S. Sempere, H. Huang, X. Sun, L. F. Nazar, *Nat. Energy* **2017**, *6*, 17119.

[25] L. Fan, H. L. Zhuang, L. Gao, Y. Lu, L. A. Archer, *J. Mater. Chem. A* **2017**, *5*, 3483.

[26] Q. Zhang, J. Pan, P. Lu, Z. Liu, M. W. Verbrugge, B. W. Sheldon, Y. T. Cheng, Y. Qi, X. Xiao, *Nano Lett.* **2016**, *16*, 2011.

[27] D. Lin, Y. Liu, W. Chen, G. Zhou, K. Liu, B. Dunn, Y. Cui, *Nano Lett.* **2017**, *17*, 3731.

[28] X. Q. Zhang, X. Chen, R. Xu, X. B. Cheng, H. J. Peng, R. Zhang, J. Q. Huang, Q. Zhang, *Angew. Chemie - Int. Ed.* **2017**, *56*, 14207.

[29] R. Xu, X. Q. Zhang, X. B. Cheng, H. J. Peng, C. Z. Zhao, C. Yan, J. Q. Huang, *Adv. Funct. Mater.* **2018**, *28*, 1.

[30] Y. Lu, Z. Tu, L. A. Archer, *Nat. Mater.* **2014**, *13*, 961.

[31] X. Q. Zhang, X. B. Cheng, X. Chen, C. Yan, Q. Zhang, *Adv. Funct. Mater.* **2017**, *27*, 1.

[32] Gordin, M. L.; Dai, F.; Chen, S.; Xu, T.; Song, J.; Tang, D.; Azimi, N.; Zhang, Z.; Wang, D. *ACS Appl. Mater. Interfaces.* 2014, 6, 8006−8010.

[33] C. Zu, N. Azimi, Z. Zhang, A. Manthiram, *J. Mater. Chem. A* **2015**, *3*, 14864.

[34] F. Marchioni, K. Star, E. Menke, T. Buffeteau, L. Servant, B. Dunn, F. Wudl, *Langmuir* **2007**, *23*, 11597.

[35] M. Wu, Z. Wen, J. Jin, B. V. R. Chowdari, *ACS Appl. Mater. Interfaces* **2016**, *8*, 16386.

[36] X. Liang, Q. Pang, I. R. Kochetkov, M. S. Sempere, H. Huang, X. Sun, L. F. Nazar, *Nat. Energy* **2017**, *6*, 17119.

[37] Q. Zhao, Z. Tu, S. Wei, K. Zhang, S. Choudhury, X. Liu, L. A. Archer, *Angew. Chemie - Int. Ed.* **2018**, *57*, 992.

[38] F. Wu, S. Thieme, A. Ramanujapuram, E. Zhao, C. Weller, H. Althues, S. Kaskel, O. Borodin, G. Yushin, *Nano Energy* **2017**, *40*, 170.

[39] F. Wu, J. T. Lee, N. Nitta, H. Kim, O. Borodin, G. Yushin, *Adv. Mater.* **2015**, *27*, 101.

[40] L. Ma, M. S. Kim, L. A. Archer, *Chem. Mater.* **2017**, *29*, 4181.

Chapter 4

Carbon tetrachloride additive for improving the self-discharge rate in ionic liquid electrolytes for lithium-sulfur batteries

Introduction

Lithium polysulfide (Li_2S_x, x = 4–8) dissolution and shuttling in liquid, ether electrolytes still remains one of the chief problems associated with lithium-sulfur (Li-S) batteries despite more than five decades worth of extensive research.[1]-[2] When long-chain polysulfides dissolve into the electrolyte, they will react with both the lithium metal anode and sulfur cathode, since polysulfides spontaneously undergo disproportionation reactions.[3] Because of this reactivity, even in a resting state, these long-chain polysulfides eventually get reduced to insoluble, short-chain polysulfides and lithium sulfide (Li_2S, Li_2S_2, Li_2S_3), which are electrically insulating and, thus, electrochemically inactive. This self-discharge from the polysulfide shuttle effect needs to be rectified in order to meet the immense economic potential promised by the adoption of Li-S batteries.[4]-[6]

Most studies attempting to suppress polysulfide dissolution have focused on cathode design. Much attention has been given to the modification of porous carbons, particularly by functionalizing their surface with heteroatoms to electrically attract polysulfides. This functionality alone, though, fails to limit the self-discharge to a commercially-viable level.[7]-[12]

Despite being one of the battery's primary components, modifications to the electrolyte have been less studied to restrict polysulfide dissolution and the self-discharge rate.[13]-[15] Among possible electrolytes, many room temperature ionic liquids (ILs) offer this property.[16]-[17] ILs are salts that are liquid at room temperature (< 100^{o}C), consisting of bulky cations and

anions that have weaker ionic bonds compared to typical salts. While these bulky ions lead to liquids that have a high viscosity (more than two orders of magnitude higher than conventional Li-S electrolyte solvents), ILs carry beneficial properties such as a high thermal stability, low volatility, a wide electrochemical window, and a wide liquidus range.

The viscosity of the electrolyte directly impacts the magnitude of Li+ ion diffusion through the electrolyte. Any study that demonstrates a Li-S cell where an IL is the sole liquid component only achieves good electrochemical performance by cycling at a low current rate.[18]-[23] Fortunately, many ILs bear strong resemblance to the supporting lithium salts (for example, lithium bis(trifluoromethanesulfonyl)imide (LiTFSI)) already employed in Li-S batteries. Therefore, rather than depending on the IL to be the sole Li^+ transport medium, IL can instead be added into common solvents such as 1-3 dioxolane (DOL) and dimethoxyethane (DME).[20]-[23] The beneficial electrochemical and safety properties of the IL are maintained even when the concentration of the IL in an IL/organic hybrid electrolyte is low.

The compatibility of ILs in Li-S batteries is highly dependent on the reactivity of the anion, showing similar trends to their conventional salt counterparts. The cation, though, impacts on some of the key electrochemical properties described previously. Anions such as hexafluorophosphate (PF_6^-), tetrafluoroborate (BF_4^-), and bis(fluorosulfonyl)amide ($[FSA]^-$) all irreversibly decompose in a polysulfide-containing environment, notably forming surface passivation films highly concentrated in lithium sulfate ($LiSO_4$) and lithium sulfide (Li_2S).[24]-[25] In contrast, these decomposition products are much less concentrated with bis(trifluoromethanesulfonyl)amide ($[TFSA]^-$). Suppressed polysulfide dissolution is also achieved thanks to the bulkiness of $[TFSA]^-$, which promotes a weak coordination ability with the Li^+ in lithium polysulfides. The cation more greatly affects the viscosity and the ionic conductivity of the solution than the polysulfide solubility. Li^+ and S_x^{2-} coordination with the cation should not be completely ignored in IL design, though, since these ions are highly reactive.[25]

Stable solid electrolyte interface (SEI) formation remains an issue when using ILs, though, since the issues related to salt decomposition are essentially the same as conventional electrolytes. To address this issue, electrolyte additives are often employed to tune the surface chemistry on the electrodes. One of the most common electrolyte additives in Li-S batteries is lithium nitrate ($LiNO_3$).[26]-[27] When cycled in the presence of polysulfides, $LiNO_3$ forms a passivation film rich in LiN_xO_y and LiS_xO_y components that limits the effects of the polysulfide shuttle effect. The benefits of $LiNO_3$ in IL electrolytes was shown by Xia *et al.* A 0% self-discharge rate was achieved after resting for 24 hours with a N-methyl-N-propylpiperidinium bis(trifluoromethanesulfonyl)imide (PP13TFSI)-based electrolyte and a $LiNO_3$ additive.[20] The polysulfide restricting effects of the IL and the passivation film formation from $LiNO_3$ combine to produce stable Li-S cycling.

Less studied with IL electrolytes is the effects of halogenated additives on the SEI. Lithium halides (LiF, LiCl, LiBr, and LiI) provide an insulating layer that establishes an ionic gradient that drives Li^+ diffusion from lithium metal to the bulk electrolyte.[28]-[34] Fast Li^+ diffusion importantly produces a uniform surface morphology that limits the formation and growths lithium "dendrites", branched agglomerations of inactive lithium metal that can cause unsafe battery operating conditions.[28], [31] Lithium halides can be introduced directly into the electrolyte or through the decomposition reactions. Our previous study described how carbon tetrachloride (CCl_4) could be reduced to LiCl in the presence of $LiNO_3$ to enable stable lithium deposition for over 400 cycles.

Based on our previous study, we studied the synergistic effects that $LiNO_3$ and CCl_4 additives bring to an IL-containing electrolyte in Li-S batteries. The IL works to mitigate polysulfide dissolution, while the additives ensure stable solid electrolyte interface formation. The IL, $LiNO_3$, and CCl_4 work together to inhibit the self-discharge rate to less than 5%, compared to

nearly 20% for conventional electrolytes. Because polysulfides, too, effect SEI formation in the presence of $LiNO_3$, restricting their dissolution emphasizes the importance of CCl_4 as an additive.

Experimental Methods

Electrolyte preprartion

Carbon tetrachloride (≥99.5%, Sigma-Aldrich) was added in varying amounts to an electrolyte of 1M lithium bis(trifluoromethanesulfonyl)imide (LiTFSI, BASF) in 2:1:1v N-propyl-N-methylpyrrolidinium bis(trifluoromethanesulfonyl)imide (99.5%, Sigma-Aldrich), 1,3-dioxolane (DOL, BASF) and 1,2-dimethoxyethane (DME, BASF) with 4 wt% lithium nitrate ($LiNO_3$, 99.99% trace metals basis, Sigma-Aldrich). A conventional electrolyte of 1M LiTFSI, 1:1v DOL/DME, and 4wt% $LiNO_3$ was also prepared to demonstrate differences in the self-discharge rate. All of the electrolyte materials were stored in an MBraun argon-filled glove box with H_2O and O_2 less than 1 ppm.

Characterization

Electrochemical and materials characterization techniques were used to gain a comprehensive understanding of the effects of carbon tetrachloride in ionic liquid electrolytes. The charge and discharge performances of Li-S batteries employing CCl_4 electrolytes were studied using Neware battery testers. Cyclic voltammetry (CV) and electrochemical impedance spectroscopy (EIS) supplemented the charge-discharge data and were conducted using a Solartron. The XRD pattern was obtained with Cu-K_α radiation on a Rigaku Miniflex II. The diffraction pattern was determined between 10-80^o 2Θ at a scan rate speed of 0.1^o per minute.

Li-S battery assembly

Li-S batteries were assembled in CR2016 coin cells with the above electrolyte. The sulfur cathode was prepared by melt-diffusing sulfur (70 wt%) into porous Ketjenblack (KB) carbon at 155ºC in a convection oven for 24 hours. After cooling to room temperature, the KB-S composite was hand-milled with Super P carbon. Finally, the powder mixture was stirred into an N-methyl-2-pyrrolidone (NMP) solvent containing the binder polyvinylidene fluorine (PVDF). The weight ratio between KB-S, Super P, and PVDF was 7:2:1. The slurry was allowed to stir for 12 hours. After stirring, the slurry was coated onto carbon-coated aluminum foil using a doctor blade. The electrode was allowed to dry first in air at room temperature for 3 hours, then in a vacuum-oven at 60ºC for 12 hours. The electrodes were then punched out into 12mm diameter discs with a sulfur loading of 1.5-2.5 mg/cm^2. Cells were assembled with these cathodes, the electrolyte described previously, a lithium metal anode, and a Celegard 2325 separator in an MBraun argon-filled glove box with H_2O and O_2 less than 1 ppm.

Results and Discussion

ILs restrict the dissolution of polysulfides into the electrolyte compared to conventional electrolytes, improving the reversibility of the Li-S reaction mechanism during cycling. Figure 4-1 shows cyclic voltammograms (CV) of Li-S cells that contain electrolytes with and without the IL (both samples contain the CCl_4 additive). Three major differences between the two samples are observed. 1) A very small decrease in the magnitude of the peaks during both the cathodic and anodic sweeps are observed with the IL. In contrast, there is a precipitous decline in these peaks when only organic components are employed as electrolyte solvents, attributed to losing active material to the electrolyte and SEI formation. The IL enables reversible reduction and oxidation

between high-order polysulfides and lithium sulfides. 2) The magnitude of the current is lower with the IL-containing electrolyte, related to obtaining a lower capacity in the initial cycles compared to the all-organic electrolyte. This is directly related to the lower Li^+ mobility in the viscous IL. 3) The second reduction peak in the first cycle appears to broaden and even split into a third peak at around 1.85 V. This could be related to both an increase cell polarization, again due to the viscosity of the IL, and the formation of a unique SEI on lithium metal. In subsequent cycles, these two peaks collapse into one peak at 2.0 V, the typical peak observed for the reduction of lower-order polysulfides to lithium sulfide.

Figure 4-1. Cyclic voltammetry of the first cycles of a Li-S cell with an ionic liquid and with only organic solvents. Both cells contained a CCl_4 additive.

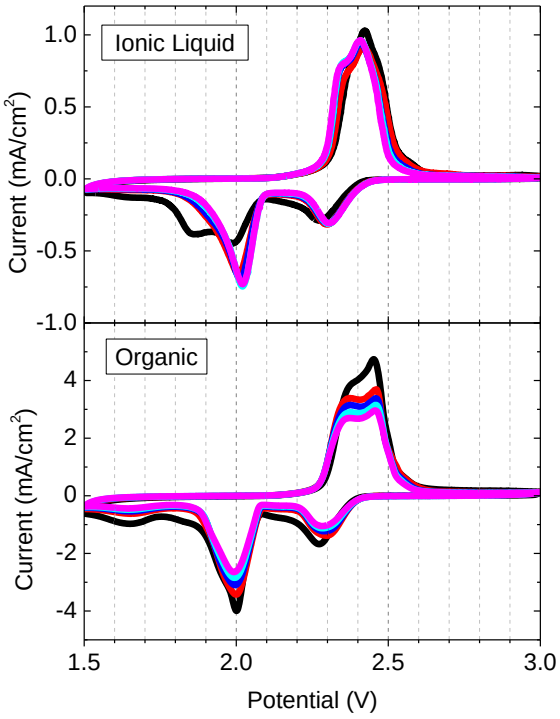

Our previous study showed how CCl_4 and $LiNO_3$ can synergistically work together to form a stable SEI layer on lithium metal, using stainless steel an electrode for lithium deposition and stripping. To properly engineer full cells, the solid electrolyte interface grown on the sulfur cathode must also be investigated, since cycling in Li-S batteries introduces new components and reactions, like lithium polysulfides. We studied the SEI on the sulfur cathode using X-ray diffraction (XRD), as shown in Figure 4-2**.** After 10 cycles, cells with the control IL electrolyte show two major features. The peaks at 26° and 27° correspond to Li_2S, while the one peak at 38° corresponds to LiF.[35]-[36] These two species are commonly in Li-S SEIs due to polysulfide reduction and LiTFSI decomposition, respectively. The IL electrolyte with the CCl_4 demonstrates two additional peaks – one at 30° and another at 35° – that can both be attributed to LiCl.[31] A properly tuned

amount of LiCl in lithium metal SEIs shows the ability to increase the Li^+ ion diffusion rate through the interphase. As an electrode, lithium metal exhibits both a high ionic and electronic conductivity, allowing for a beneficial Li^+ gradient to form. The sulfur cathode, on the other hand, is much less conductive due in large part to the insulating nature of sulfur itself. Adding insulating materials to the SEI causes an increase in cell polarization, demonstrating the engineering tradeoff when employing LiCl and similar materials for lithium metal protection.

Figure 4-2. X-ray diffraction (XRD) patterns of sulfur cathode surfaces after 10 cycles of Li-S batteries with an IL electrolyte with and without a CCl_4 additive.

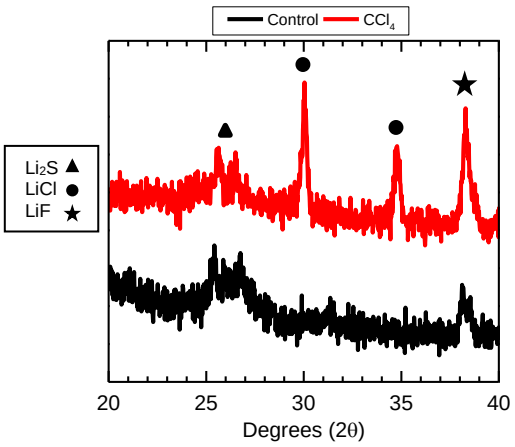

The dissolution of polysulfides leads to a high rate of self-discharge due to their ability to react with both electrodes and to disproportionate with one another. This phenomenon can be illustrated through a number of electrochemical characterization techniques. Figure 4-3 illustrates cells cycled in conventional electrolyte at 0.5C, where the cells were rested for 24 hours after the 10^{th}, 20^{th}, and 30^{th} cycles, then cycled continuously thereafter. As shown in a previous study, 50mM CCl_4 was determined to be the optimum concentration for this additive for long-term battery cycling due to its ability to form LiCl and protect lithium metal anodes. During all three rest periods, the capacity drops at least 15% with or without CCl_4, illustrating the effects of polysulfide dissolution on Li-S battery performance. CCl_4, though, does a better job of limiting the rate of self-discharge. The change in the capacity difference decreases after each successive resting stage (18.4% to 17.9% to 15.4%), which suggests that the engineered SEI protection layer limits the reactivity of the polysulfides with lithium metal. This is in clear contract to cells that only employed $LiNO_3$ to form

Figure 4-3. Self-discharge cycling performance in Li-S cells using DOL/DME electrolytes with a CCl_4 additive, tested at a 0.5C current rate. The inset illustrates the corresponding Coulombic efficiency between cycles 5 and 35.

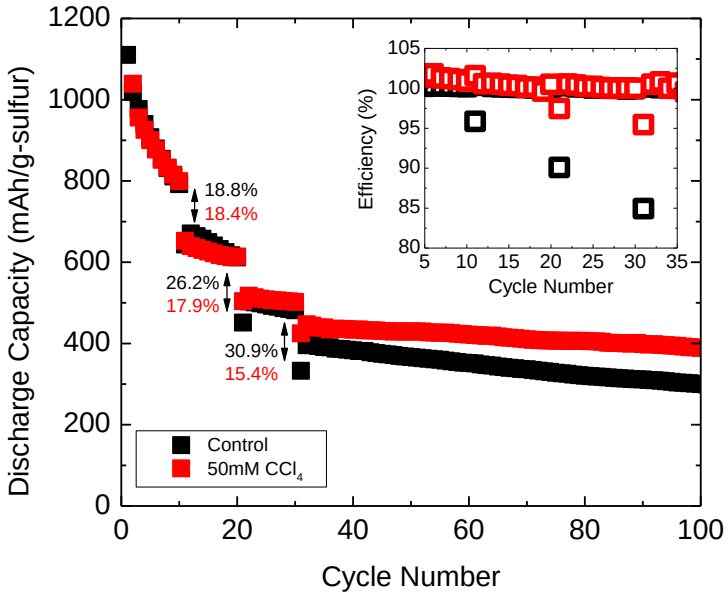

a protective layer, where the change in the capacity difference increased after each resting stage (18.8% to 26.2% to 30.9%). Additionally, the Coulombic efficiency (CE) was 101.6%, 97.5%, and 95.5% after the three rest phases with the CCl_4, significantly higher than the 95.9%, 90.1%, and 84.9% efficiencies demonstrated by the control electrolyte. The electrochemical reduction of CCl_4 itself could be responsible for a portion of the improvements in both the capacity and CE, but the rate of capacity fading and the percent drop in the CE in subsequent rest periods demonstrates how the byproducts of this electrochemical reduction improve battery performance. Cells with CCl_4 maintain a capacity of 389 mAh/g after 100 cycles, losing 12.4% of their capacity from the final rest period. Again, this is a stark contrast to solely using $LiNO_3$ as a SEI passivation layer, where cells obtained a capacity of just 300 mAh/g and lost 24.1% of their capacity from the final rest period. Nonetheless, even with the additive, these electrochemical experiments demonstrate how Li-S batteries suffer major self-discharge in conventional electrolytes.

The same charge-discharge tests were then repeated using IL-containing electrolytes to illustrate how IL demonstrate improved performance. The voltage profile, shown in Figure 4-4a, shows the characteristic two plateaus upon discharge, the upper one attributed to elemental sulfur being reduced to long-chain polysulfides (Li_2S_x, x = 4–8) and the lower one attributed to those long-chain polysulfuides being reduced to short-chain sulfides (Li_2S_x, x = 1–3). The CE of the first cycle

with the CCl_4 additive is 113%, suggesting that CCl_4 reacts with lithium polysulfides/sulfides or its byproducts, like lithium sulfate (Li_2SO_4). Previously, we demonstrated how CCl_4 reacts with $LiNO_3$ in the presence of lithium metal; another study showed how $SiCl_4$ reacts with carbonates; therefore, a similar reaction could potentially occur between CCl_4 and Li_2SO_4. The first cycle is the only one with a CE much greater than 100%, further demonstrating that CCl_4 is primarily involved in SEI formation. Additionally, charge-discharge voltage hysteresis is slightly higher when using the CCl_4 additive. The increased resistance experienced by Li-S cells with the CCl_4 additive is also reflected by electrochemical impedance spectroscopy (EIS), as shown in Figure 4-4b.[37] Our previous study showed a lower voltage hysteresis through the SEI on lithium metal with the chlorinated additive, but that study did not include polysulfides; therefore, the reaction between CCl_4 and polysulfides is likely the source of the increased hysteresis/resistance in the Li-S cell.

Despite this increased resistance in the cell, battery performance is still improved using the CCl_4 additive due to improved lithium metal protection. Figure 4-4c shows the cycling and CE of Li-S cells, tested under the same current rate as those with organic electrolytes. The initial capacity for cells with and without a CCl_4 additive was 832 mAh g^{-1} and 890 mAh g^{-1}, respectively, significantly lower than without the IL. The higher viscosity of the IL lowers the Li^+ mobility through the electrolyte and increases the voltage polarization. Nevertheless, IL-containing electrolytes show more stable long-term battery performance. After 100 cycles, the capacity is nearly double that of the conventional electrolytes, with the CCl_4 additive electrolyte demonstrating a 638 mAh g^{-1} specific capacity compared to 551 mAh g^{-1} without CCl_4. Focusing on the self-discharge test cycles, cells with CCl_4 demonstrate a 4.0%, 7.2%, and 4.6% capacity fading after resting for 24 hours after the 10^{th}, 20^{th}, and 30^{th} cycles, respectively, while cells without CCl_4 demonstrate a 4.9%, 9.2% and 8.6% capacity fading. The capacity fading after these self-discharge tests is also decreased with the chlorinated additive, illustrating the effectiveness of CCl_4 in improving the SEI on lithium metal.

Figure 4-4. a) The 1st, 30th, and 31st charge-discharge voltage profile for IL electrolytes without (top) and with (bottom) a CCl_4 additive. The cell was rested for 24 hours between the 30th and 31st cycles. b) Electrochemical impedance spectroscopy of selected cycles for a Li-S cell using an IL electrolyte without (left) and with a CCl_4 additive (right). c) The specific capacity of Li-S cells at a 0.5C current rate, with 24 hour rests after 10, 20, and 30 cycles. The inset illustrates the corresponding Coulombic efficiency between cycles 8 and 36.

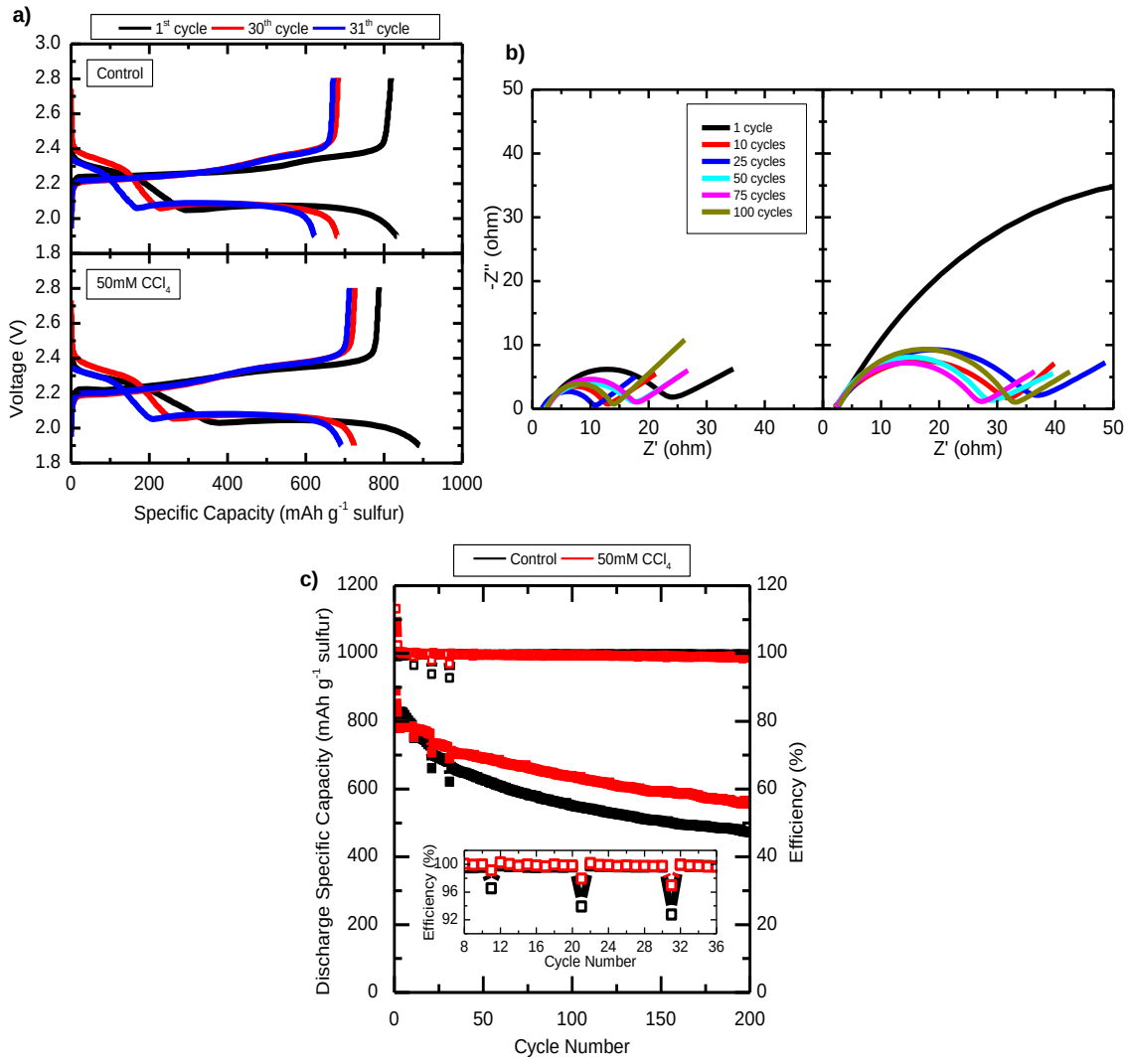

Conclusion

Ionic liquids limit polysulfide dissolution through both their physical and chemical properties, while offering improved safety over electrolytes with only ether solvents. Additives improve the solid electrolyte interface on lithium metal to ensure uniform Li deposition, limiting

the formation of dendrites. Lithium nitrate and carbon tetrachloride work synergistically in an ionic-liquid-containing electrolyte to form a stable SEI layer that limits the self-discharge rate of Li-S batteries. After resting for 24 hours after 10, 20, and 30 cycles, the capacity fading was 4.0%, 7.2%, and 4.6%, for Li-S cells with both $LiNO_3$ and CCl_4 additives. The benefits of this protective layer on the lithium metal anode appear to outweigh the costs of adding the same insulating layer to the SEI on the sulfur cathode, whereby the overall resistance of the cell is increased. This study demonstrates the profound impact that proper lithium metal protection can have on full cell performance. More research attention should be devoted to this area to realize the economic potential of Li-S batteries.

References

[1] Y.-X. Yin, S. Xin, Y.-G. Guo, L.-J. Wan, *Angew. Chem. Int. Ed. Engl.* **2013**, *52*, 13186.

[2] E. P. Kamphaus, P. B. Balbuena, *J. Phys. Chem. C* **2016**, *120*, 4296.

[3] Y. V. Mikhaylik, J. R. Akridge, *J. Electrochem. Soc.* **2004**, *151*, A1969.

[4] Y. Diao, K. Xie, S. Xiong, X. Hong, *J. Electrochem. Soc.* **2012**, *159*, A421.

[5] Z. Ma, X. Huang, Q. Jiang, J. Huo, S. Wang, *Electrochim. Acta* **2015**, *182*, 884.

[6] C. Barchasz, F. Molton, C. Duboc, J. Lepretre, S. Patoux, F. Alloin, *Anal. Chem.* **2012**, *84*, 3973.

[7] J. P. Paraknowitsch, A. Thomas, *Energy Environ. Sci.* **2013**, *6*, 2839.

[8] X. Ji, L. Nazar, *J. Mater. Chem.* **2010**, *20*, 9821.

[9] A. Ghosh, S. Shukla, G. S. Khosla, B. Lochab, S. Mitra, *Sci. Rep.* **2016**, *6*, 25207.

[10] J. Song, M. L. Gordin, T. Xu, S. Chen, Z. Yu, H. Sohn, J. Lu, Y. Ren, Y. Duan, D. Wang, *Angew. Chemie - Int. Ed.* **2015**, *54*, 4325.

[11] J. Song, Z. Yu, M. L. Gordin, D. Wang, *Nano Lett.* **2016**, *16*, 864.

[12] T. Z. Hou, X. Chen, H. J. Peng, J. Q. Huang, B. Q. Li, Q. Zhang, B. Li, *Small* **2016**, 3283.

[13] M. L. Gordin, F. Dai, S. Chen, T. Xu, J. Song, D. Tang, N. Azimi, Z. Zhang, D. Wang, *ACS Appl Mater Interfaces* **2014**, *6*, 8006.

[14] S. Chen, F. Dai, M. L. Gordin, Z. Yu, Y. Gao, J. Song, D. Wang, *Angew. Chemie - Int. Ed.* **2016**, *55*, 4231.

[15] S. Chen, Y. Gao, Z. Yu, M. L. Gordin, J. Song, D. Wang, *Nano Energy* **2017**, *31*, 418.

[16] C. Zu, N. Azimi, Z. Zhang, A. Manthiram, *J. Mater. Chem. A* **2015**, *3*, 14864.

[17] M. Watanabe, M. L. Thomas, S. Zhang, K. Ueno, T. Yasuda, K. Dokko, *Chem. Rev.* **2017**, *117*, 7190.

[18] J. W. Park, K. Ueno, N. Tachikawa, K. Dokko, M. Watanabe, *J. Phys. Chem. C* **2013**, *117*, 20531.

[19] K. Dokko, N. Tachikawa, K. Yamauchi, M. Tsuchiya, A. Yamazaki, E. Takashima, J.-W. Park, K. Ueno, S. Seki, N. Serizawa, M. Watanabe, *J. Electrochem. Soc.* **2013**, *160*, A1304.

[20] L. Wang, J. Liu, S. Yuan, Y. Wang, Y. Xia, *Energy Environ. Sci.* **2016**, *9*, 224.

[21] S. Xiong, J. Scheers, L. Aguilera, D.-H. Lim, K. Xie, P. Jacobsson, A. Matic, *RSC Adv.* **2015**, *5*, 2122.

[22] J. Zheng, M. Gu, H. Chen, P. Meduri, M. H. Engelhard, J.-G. Zhang, J. Liu, J. Xiao, *J. Mater. Chem. A* **2013**, *1*, 8464.

[23] S. Xiong, K. Xie, E. Blomberg, P. Jacobsson, A. Matic, *J. Power Sources* **2014**, *252*, 150.

[24] N. S. Manan, L. Aldous, Y. Alias, P. Murray, L. J. Yellowlees, M. C. Lagunas, C. Hardacre, *J Phys Chem B* **2011**, *115*, 13873.

[25] G. Bieker, J. Wellmann, M. Kolek, K. Jalkanen, M. Winter, P. Bieker, *Phys Chem Chem Phys* **2017**, *19*, 11152.

[26] D. Aurbach, E. Pollak, R. Elazari, G. Salitra, C. S. Kelley, J. Affinito, *J. Electrochem. Soc.* **2009**, *156*, A694.

[27] W. Li, H. Yao, K. Yan, G. Zheng, Z. Liang, Y.-M. Chiang, Y. Cui, *Nat. Commun.* **2015**, *6*, 7436.

[28] Q. Zhang, J. Pan, P. Lu, Z. Liu, M. W. Verbrugge, B. W. Sheldon, Y. T. Cheng, Y. Qi, X. Xiao, *Nano Lett.* **2016**, *16*, 2011.

[29] X. Q. Zhang, X. Chen, R. Xu, X. B. Cheng, H. J. Peng, R. Zhang, J. Q. Huang, Q. Zhang, *Angew. Chemie - Int. Ed.* **2017**, *56*, 14207.

[30] D. Lin, Y. Liu, W. Chen, G. Zhou, K. Liu, B. Dunn, Y. Cui, *Nano Lett.* **2017**, *17*, 3731.

[31] X. Liang, Q. Pang, I. R. Kochetkov, M. S. Sempere, H. Huang, X. Sun, L. F. Nazar, *Nat. Energy* **2017**, *6*, 17119.

[32] F. Marchioni, K. Star, E. Menke, T. Buffeteau, L. Servant, B. Dunn, F. Wudl, *Langmuir* **2007**, *23*, 11597.

[33] F. Wu, S. Thieme, A. Ramanujapuram, E. Zhao, C. Weller, H. Althues, S. Kaskel, O. Borodin, G. Yushin, *Nano Energy* **2017**, *40*, 170.

[34] F. Wu, J. T. Lee, N. Nitta, H. Kim, O. Borodin, G. Yushin, *Adv. Mater.* **2015**, *27*, 101.

[35] X. B. Cheng, R. Zhang, C. Z. Zhao, Q. Zhang, *Chem. Rev.* **2017**, *117*, 10403.

[36] Y. Sakamura, M. Iizuka, S. Kitawaki, A. Nakayoshi, H. Kofuji, *J. Nucl. Mater.* **2015**, *466*, 269.

[37] J. Luo, R. Lee, J. Jin, Y. Weng, C. Fang, *Chem. Commun.* **2017**, *53*, 963.

Chapter 5

Conclusion

Lithium-ion batteries (LIBs) enabled the development of many modern day portable electronic devices. They have also been used in many of all-electric vehicles developed recently, but their impact on this market is severely limited since their energy density does not allow for long-range driving. Additionally, the active materials in LIBs contain rare metals, which makes them expensive. The lithium-ion, Li^+, the second smallest positively charged monovalent ion, which makes it particularly attractive for batteries that demand fast ion transport. The next big advance in batteries will likely incorporate lithium in some form.

One extensively studied next generation lithium-based battery is lithium-sulfur (Li-S). Lithium metal, the anode material in this configuration, has the lowest weight and density of all metals, while also possessing the lowest electrochemical potential of all known materials. Both of these properties could lead to large increases in energy density if properly engineered. Sulfur, the cathode material, is both naturally abundant and an underutilized industrial waste product, making it a significantly more cost-effective than current LIB cathodes. Additionally, the specific capacity of sulfur is more than 10 times greater than transition metal oxides. Combined together, the theoretical energy density of Li-S batteries is approximately six times higher than that of today's LIBs. Such an increase in energy density combined with the drop in price for the active materials would remake the entire personal vehicle market, making all-electric vehicles highly competitive with gasoline powered internal combustion engines. This would not only be beneficial in terms of economics, but also in terms of the environment, as the need for clean, renewable energy storage becomes necessary in the face of climate change.

While more than five decades of research has been dedicated to commercializing Li-S batteries, commercialization and widespread adoption still appear to be years away. The

fundamental chemical properties of both sulfur and lithium metal do not naturally make them high performing battery materials. Sulfur and lithium sulfide, the end product the electrochemical reduction of sulfur, are electronic insulators. This greatly effects the energy density that can be achieved, since less electrochemically active materials need to be added to improve the electronic conduction pathways in the cathode. Active material is also lost through polysulfide dissolution and the polysulfide shuttle effect. When rested for extended periods of time, Li-S batteries lose much of their capacity due to these phenomena. As for the lithium metal anode, the challenge comes from its reactivity and forming a uniform solid electrolyte interface (SEI) on its surface. Ether electrolyte solvents and conductive lithium salts decompose upon contact with lithium metal. Their decomposition products unevenly distribute within the SEI, creating potential gradients on the surface where lithium preferentially agglomerates. Over the course of cycling, these inactive lithium agglomerations grow into structures known as "dendrites" that easily short-circuit the battery.

The SEI on lithium metal can be engineered through electrolyte additives. My work studied the structure-property relationships of the SEI with high-sulfur content and high-chlorine content electrolyte additives. First, I showed how a high sulfur content polymer based on 1,2,3-trichloropropane (TCP) provides both organic and inorganic component to the SEI, forming a stable film. TCP-S_8 (83.7 wt% sulfur), synthesized via a facile emulsion technique, demonstrated a 97.3% average Coulombic efficiency over 350 cycles and >90% efficiency through 400 cycles at a current density of 2 mA cm^{-2} and a deposition capacity of 1 mAh cm^{-2}. Compared to SEIs with only inorganic polysulfide, TCP-S_8 lowered the average voltage hysteresis by 100 mV. The SEI contained no noticeable breaks, a significantly contrast to the control electrolyte. Second, a highly-chlorinated additive, carbon tetrachloride, decomposes on lithium metal to form a hybrid SEI consisting of inorganic lithium chloride and a carbon-centric, nitrate containing polymer. At an optimized concentration of 50mM, the electrolyte with a CCl_4 additive achieved an average

columbic efficiency of 98.3% over the first 300 cycles and remained at above 90% for nearly 450 cycles. The SEI components from the additive improve lithium metal deposition and restrict the formation of lithium dendrites. Finally, carbon tetrachloride was employed added into an ionic liquid electrolyte to show how restricted polysulfide dissolution and improved lithium metal protection contribute to improved Li-S battery performance. After resting for 24 hours after 10, 20, and 30 cycles, the capacity fading was 4.0%, 7.2%, and 4.6%, for Li-S cells with both $LiNO_3$ and CCl_4 additives. Li-S cells with these additives demonstrated a 638 mAh g^{-1} specific capacity at a 0.5C current rate, nearly double the performance of conventional ether electrolytes.

These studies all investigated the beneficial, fundamental changes that high-sulfur content and high-chlorine content materials contribute to the SEI. One area that warrants further investigation is the effects of these additives on SEI formation and battery performance in an electrolyte-lean environment. Many studies, including the ones presented in this dissertation, use excess electrolyte to negate any issues associated with electrode wetting (for example, activing the sulfur cathode) and ionic conductivity; however, the electrolyte is often the heaviest component of the battery, which means the volume added needs to be limited to achieve commercially viable energy densities. Lowering the electrolyte to active material ratio could lead to profound increases in energy density. Nevertheless, studies with excess electrolyte help to elucidate important electrolyte decomposition mechanisms. This dissertation demonstrated those mechanisms and their effects on the SEI on lithium metal anodes with high-sulfur and high-chlorine content additives, an important building block for realizing the immense potential of Li-S batteries.

Appendix A

Supplementary Information - Trichloropropane-based sulfur polymer interlayer improves the columbic efficiency of lithium-sulfur batteries

Supplementary Figure A-1. A representative field-emission scanning electron microscopy (FESEM) image of the sulfur-rich TCP-S_x polymers.

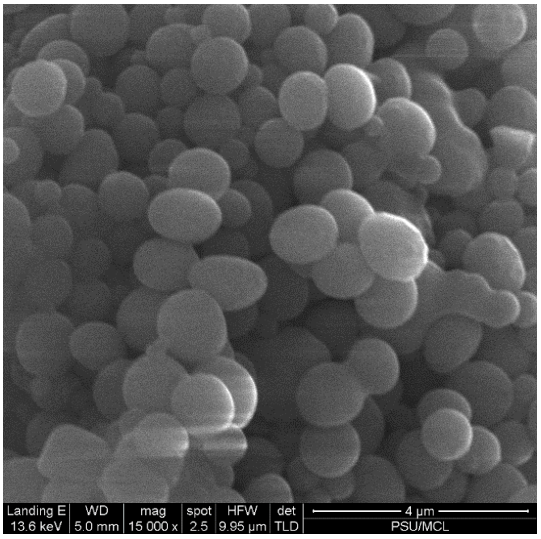

Supplementary Figure A-2. X-ray diffraction patterns for sulfur and TCP-S_x polymers.

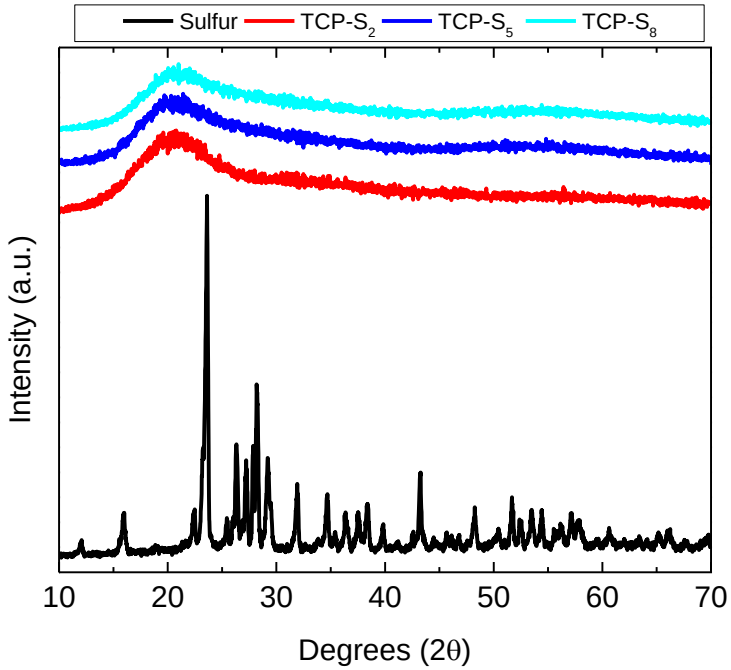

Supplementary Table A-1. Elemental analysis of the TCP-S_x polymers.

Sample	Sulfur	Carbon	Hydrogen	Nitrogen	Chlorine
TCP-S_2	61.92%	26.29%	3.62%	0.43%	1.04%
TCP-S_5	79.70%	13.49%	1.45%	< 0.02%	0.26%
TCP-S_8	83.70%	9.62%	0.74%	< 0.02%	0.25%

Supplementary Figure A-4. Fourier-transform infrared (FTIR) spectroscopy of (a) sulfur, (b) 1,2,3-trichloropropane, (c) TCP-S_2, (d) TCP-S_5, and (e) TCP-S_8.

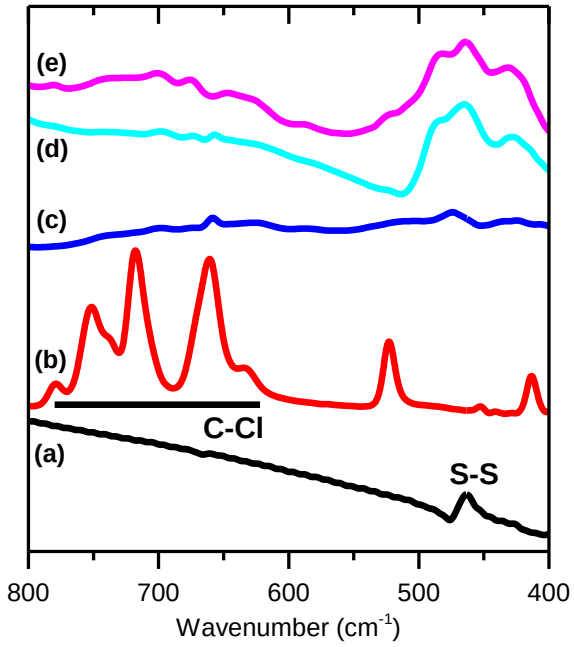

Appendix B

Supplementary Information - A synergistic lithium metal solid-electrolyte interface with carbon tetrachloride and lithium nitrate for lithium-sulfur batteries

The electrochemical stability of the SEI was also studied with di-substituted and tri-substituted chlorinated hydrocarbons: 1,6-dichlorohexane (DCH), 1,8-dichlorooctane (DCO), 1,10-dichlorooctane (DCO) and 1,2,3-trichloroproane (TCP). Regardless of concentration, the di-substituted hydrocarbons demonstrated worse electrochemical performance than the control sample. The most likely explanation for this behavior is the di-substituted molecules did not react with the nitrates or carbonates, instead behaving as a bulky, insoluble additive that exacerbated the potential gradients on lithium metal. In contrast, the tri-substituted additive, TCP, performed better than the control sample when the concentration was optimized in the electrolyte, likely following a similar mechanism to CCl_4.

Supplementary Figure B-1. The electrochemical performance of various di-substituted and tri-substituted electrolyte additives. The deposition capacity was 1 mAh cm-2 and the current density was 2 mA cm-2.

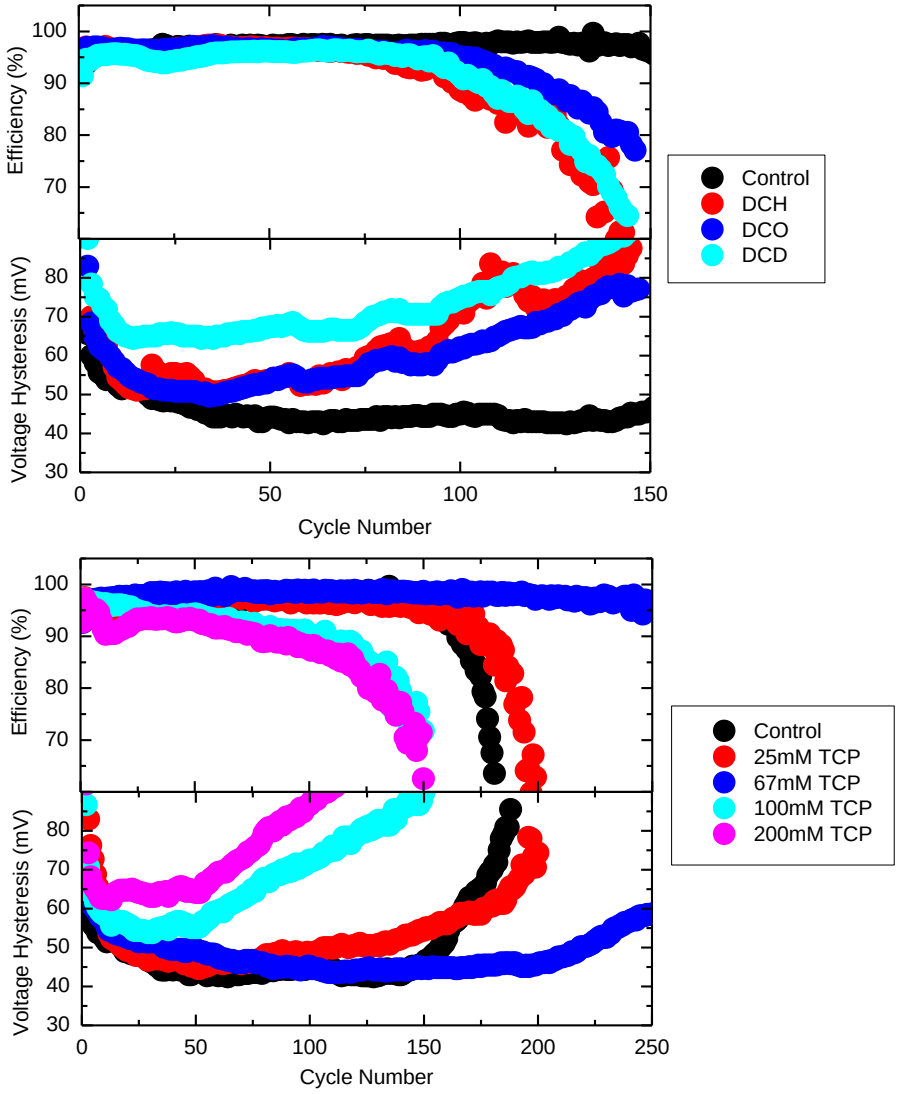

Supplementary Figure B-2. The voltage profile of the 100th cycle of lithium deposition and stripping in the two-electrode cell. The inset illustrates the region of the voltage profile used to determine the voltage hysteresis.

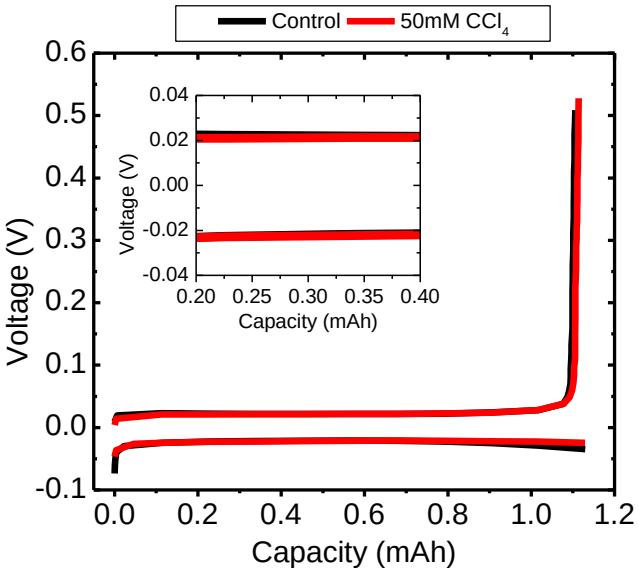

Supplementary Figure B-3. The coulombic efficiency of a Li/stainless steel cell containing an electrolyte with 50mM CCl_4, but no $LiNO_3$. The deposition capacity was 1 mAh cm^{-2} and the current density was 2 mA cm^{-2}.

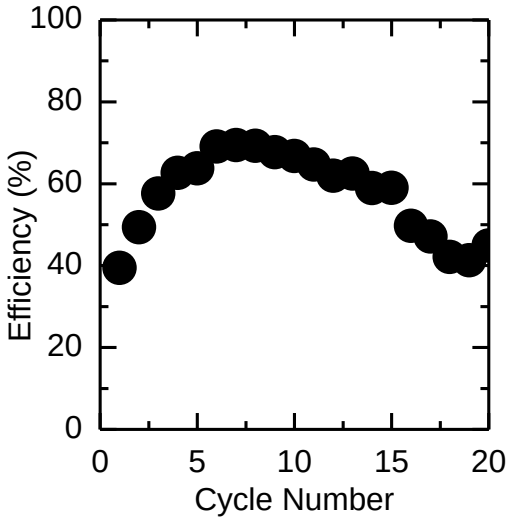

VITA

Michael Regula

EDUCTATION

Penn State University University Park, PA
Ph.D. in Chemical Engineering under Dr. Donghai Wang
Diefenderfer Graduate Fellowship

Penn State University University Park, PA
B.S. in Chemical Engineering (specialization in Energy & Fuels)
Minor in Chemistry

PUBLICATIONS & PRESENTATIONS

M. Regula, D. Wang, Sulfur-rich and chlorine-rich materials to protect lithium metal anodes, *Penn State Energy Days Conference*, **2018** (poster presentation)

S. Xiong, **M. Regula**, D. Wang, J. Song, Towards Better Lithium-Sulfur Batteries: Functional Non-Aqueous Liquid Electrolytes, *Electrochemical Energy* Reviews, accepted, **2018**

M. Regula, D. Wang, Improved Solid Electrolyte Interface on Lithium Metal Using High-Sulfur-Content Polymers, *232nd ECS Meeting*, **2017** (oral presentation)

M. Regula, D. Wang, Protecting lithium metal anodes with sulfur-rich polymers, *Millennium Café at Penn State*, **2017** (oral presentation)

S. A. Akhade, N. J. Bernstein, M. R. Esopi, **M. Regula**, M. J. Janik, A simple method to approximate electrode potential-dependent activation energies using density functional theory, *Catalysis Today*, **2017**.

H. Sohn, M. L. Gordin, **M. Regula**, D. H. Kim, Y. S. Jung, J. Song, D. Wang, Porous spherical polyacrylonitrile-carbon nanocomposite with high loading of sulfur for lithium-sulfur batteries, *J. Power Sources*, **2016**, 302, 70.

J. Song, Z. Yu, M. L. Gordin, S. Hu, R. Yi, D. Tang, T. Walter, **M. Regula**, D. Choi, X. Li, A. Manivannan, D. Wang, Chemically bonded phosphorus/graphene hybrid as a high performance anode for sodium-ion batteries, *Nano Letters*, **2014**, *14*, 6329.
J. Song, M. Zhou, R. Yi, T. Xu, M. L. Gordin, D. Tang, Z. Yu, **M. Regula**, D. Wang, Interpenetrated Gel Polymer Binder for High-Performance Silicon Anodes in Lithium-ion Batteries, *Adv. Funct. Materials*, **2014**, *24*, 5904.

J. Song, Z. Yu, T. Xu, S. Chen, H. Sohn, **M. Regula**, D. Wang, Flexible freestanding sandwich-structured sulfur cathode with superior performance for lithium–sulfur batteries, *J. Mater. Chem. A*, **2014**, *2*, 8623.